Chapter 4
Porous Copper Electrodes Formed by the Constant and the Periodically Changing Regimes of Electrolysis

Nebojša D. Nikolić

4.1 Introduction

The formation of open and porous structures with extremely large surface area is of high technological significance, because this structure type is very suitable for electrodes in many electrochemical devices, such as fuel cells, batteries and sensors [1, 2], and in catalysis applications [3]. The template-directed synthesis method is most commonly used for the preparation of such electrodes. This method is based on a deposition of desired materials in interstitial spaces of disposable hard template. When interstitial spaces of template are filled by deposited material, the template is removed by combustion or etching, and then the deposited material with the replica structure of the template is obtained [4, 5]. The most often used hard templates are porous polycarbonate membranes [6, 7], anodic alumina membrane [8–10], colloidal crystals [11, 12], echinoid skeletal structures [13], and polystyrene spheres [14, 15].

N.D. Nikolić (✉)
ICTM-Institute of Electrochemistry, University of Belgrade,
Njegoseva 12, P.O.B. 473,11001 Belgrade, Serbia
e-mail: nnikolic@tmf.bg.ac.rs

Stojan S. Djokić (ed.), *Electrochemical Production of Metal Powders*, Modern Aspects of Electrochemistry 54, DOI 10.1007/978-1-4614-2380-5_4,

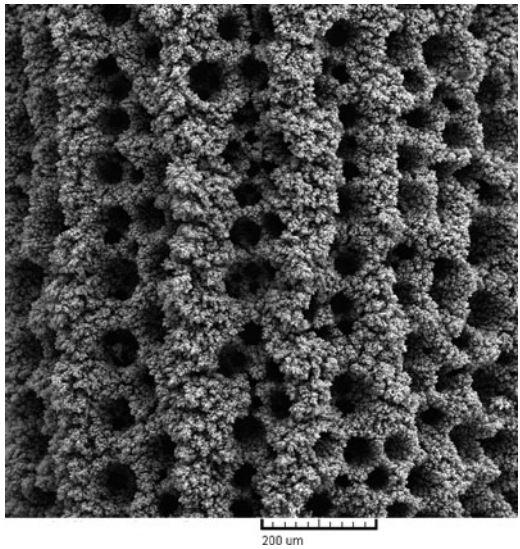

Fig. 4.1 The honeycomb-like structure formed by electrodeposition from 0.15 M $CuSO_4$ in 1.0 M H_2SO_4 at an overpotential of 1,000 mV with a quantity of the electricity 10 mAh/cm^2 (Reprinted from [22] with permission from Elsevier and [23] with permission from Springer.)

Electrodeposition technique showed as very favorable way for the production of porous electrodes [1, 2, 4]. The open porous copper and copper–tin alloys electrodes, denoted as both 3-D foam [1, 2, 4] and honeycomb-like ones [16–23], are formed by electrodeposition at high current densities and overpotentials, where parallel to electrodeposition process, the hydrogen evolution reaction occurs. The main characteristics of these electrodes are holes or pores formed by attached hydrogen bubbles surrounded by metals grain agglomerates or dendritic particles (Fig. 4.1). This way of preparing porous electrodes is denoted as gas bubble dynamic template method, where the hydrogen bubbles function as a dynamic template for the formation of this type of deposits. The advantage of producing porous materials by this hydrogen bubble dynamic template method when compared with hard template methods is its low cost, ease of preparation, facile control of structure, and facile one-step synthesis process, including preparation of the template, metal deposition, and elimination of the template [5].

4.2 Potentiostatic Regime of Electrolysis

In potentiostatic regimes of electrolysis, honeycomb-like copper electrodes are formed by electrochemical deposition at overpotentials outside the plateau of the limiting diffusion current density where the parallelism between copper electrodeposition rate and hydrogen evolution reaction is evident [16, 23]. Hydrogen evolution responsible for the formation of the honeycomb-like electrodes was vigorous enough to cause such stirring of the copper solution which leads to the decrease of the cathode diffusion layer thickness and to the increase of the limiting diffusion current density and hence to the change of the hydrodynamic conditions in the near-electrode layer [16]. For copper solutions containing 0.15 M $CuSO_4$ and less (in 0.50 M H_2SO_4), the critical quantity of evolved hydrogen leading to a change of hydrodynamic conditions in the near-electrode layer was estimated to correspond to the average current efficiency of hydrogen evolution of 10.0% [20].

4.2.1 Phenomenology of Formation of the Honeycomb-Like Structures

The formation of porous deposits by dynamic template method can be briefly presented as follows: in the initial stage of the electrodeposition process, both the nuclei of deposited metal and the "nuclei" of hydrogen bubbles are formed at the active sites of the electrode surface (Fig. 4.2a) [18]. The hydrogen bubbles isolate the substrate and then the current lines are concentrated around them making rings consisted of agglomerates of grains of deposited metal. The current lines are also concentrated at the metal nuclei formed in the initial stage between the hydrogen bubbles forming copper grains agglomerates of them. In the growth process, due to current density distribution effect, both hydrogen evolution and copper nucleation primarily occur at top of these agglomerates. Some of the new, freshly formed hydrogen bubbles will coalesce with hydrogen bubbles formed in the initial stage of electrodeposition process, leading to their growth with

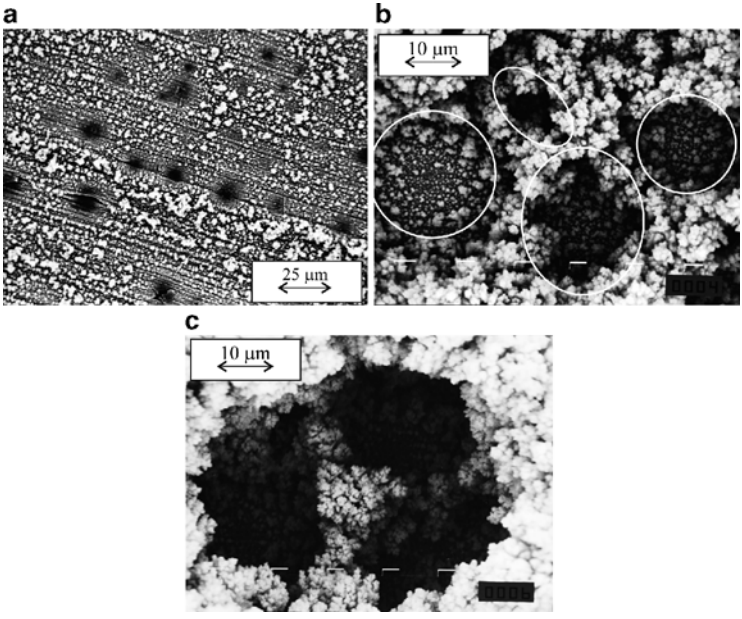

Fig. 4.2 Copper deposits electrodeposited from 0.15 M $CuSO_4$ in 0.50 M H_2SO_4 at an overpotential of 1,000 mV. Time of electrolysis: (**a**) 10 s; (**b**) 30 s, and (**c**) 120 s (Reprinted from [18, 23] with permission from Springer.)

electrolysis time. When the critical size of these hydrogen bubbles to detach from electrode surface is reached, they will detach from electrode surface forming holes of regular shapes at electrode surface. This "regular" type of holes is shown in Fig. 4.2b in circle. Simultaneously, holes of irregular shape are formed at electrode surface of agglomerate copper grains formed between hydrogen bubbles [18]. These "irregular" holes are situated between regular holes, and they are shown in Fig. 4.2b in ellipse. For longer electrodeposition time, coalescence of closely formed hydrogen bubbles occurs, leading to the formation of large so-called coalesced holes (Fig. 4.2c) [18].

Meanwhile, some of the new, freshly formed hydrogen bubbles will not coalesce with the previously formed hydrogen bubbles because

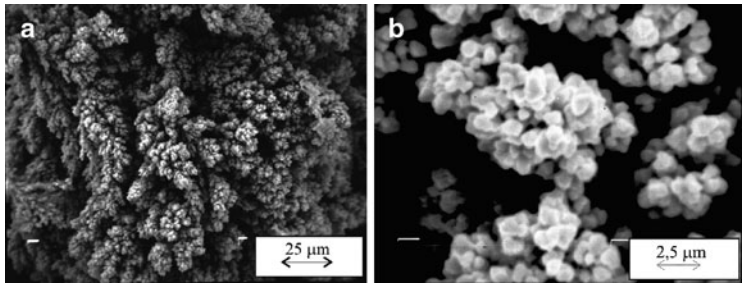

Fig. 4.3 Copper deposits electrodeposited from 0.075 M $CuSO_4$ in 0.50 M H_2SO_4 at an overpotential of 1,000 mV. Quantity of electricity: 20 mAh/cm^2 (Reprinted from [19] with permission from Elsevier and [23] with permission from Springer.)

they are situated between the freshly formed copper nucleus and these hydrogen bubbles have not enough place to develop in large hydrogen bubbles. These hydrogen bubbles will detach very fast from the electrode surface forming a channel structure through the interior of the deposit [19]. The typical channel structure formed by simultaneous hydrogen evolution and copper nucleation is shown in Fig. 4.3a. The "top view" of the part of the honeycomb-like structure shown in Fig. 4.3a is given in Fig. 4.3b; from it can be seen cauliflower-like agglomerates of copper grains surrounded by irregular channels for which the origin is of evolved hydrogen.

All elements constructing the honeycomb-like structure can also be seen from Fig. 4.4 showing a cross section of this type of deposit [24].

The "regular holes" formed by both the attached hydrogen bubbles (part in circle denoted with *A* in Fig. 4.4a) and the coalescence of neighboring hydrogen bubbles (part in circle denoted with *B* in Fig. 4.4a) and "irregular holes" formed due to the effect of current distribution at the growing surface (parts denoted by arrow labeled *C* in Fig. 4.4a) are shown in Fig. 4.4a [24]. The presence of channel structures formed through the interior of the deposit can be easily observed by cross section analysis of this deposit at a higher magnification (Fig. 4.4b).

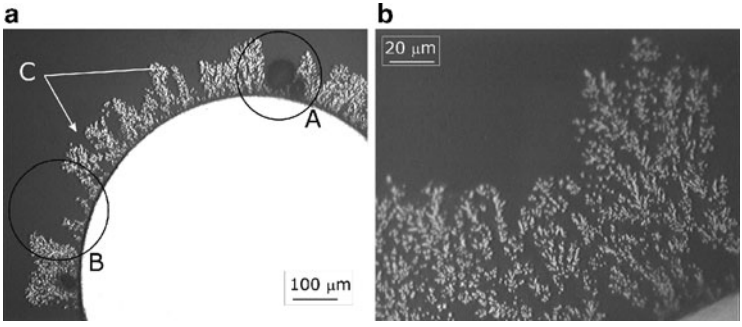

Fig. 4.4 Cross section of copper deposit electrodeposited from 0.15 M $CuSO_4$ in 0.50 M H_2SO_4, at an overpotential of 1,000 mV with a quantity of the electricity of 10 mAh/cm^2 (Reprinted from [24] with permission from Serbian Chemical Society.)

4.2.2 Parameters Affecting Number, Size and Distribution of Holes in the Honeycomb-Like Structures

Electrodeposition technique is a suitable way to get open and porous structure because it is very easy to control number, size and distribution of holes by the choice of appropriate electrodeposition conditions [19].

Factors affecting number, size, and distribution of holes are:

(a) Overpotential of electrodeposition
(b) Preparation of working electrode
(c) Concentration of Cu(II) ions
(d) Concentration of sulfuric acid
(e) Temperature of electrolysis
(f) Time of electrolysis

4.2.2.1 Overpotential of Electrodeposition

Increasing the overpotential intensifies hydrogen evolution reaction [16, 23]. For copper solution containing 0.15 M $CuSO_4$ in 0.50 M H_2SO_4, the average current efficiency of hydrogen evolution, $\eta_{I,av}(H_2)$, was about three times larger at an overpotential of 1,000 mV ($\eta_{I,av}(H_2) = 30.0\%$) than at 800 mV ($\eta_{I,av}(H_2) = 10.8\%$) [16]. It is manifested by the

formation of the honeycomb-like structures with the considerably larger number of holes formed of detached hydrogen bubbles at 1,000 mV than at 800 mV.

4.2.2.2 Preparation of Working Electrode

The number, size, and distribution of holes in the honeycomb-like electrodes strongly depended on the type of working electrode used for copper electrodeposition [17, 18]. The strong difference in the initial stage of their formation, as well as in the formed honeycomb-like structures, was observed in the dependence of the type of used working electrode. The number of hydrogen bubbles formed at the electrode with large number of active centers, where irregularities at electrode surface represent active centers for the formation of both the hydrogen bubbles and agglomerates of copper grains, was several times higher than the number of holes formed at the electrode with "killed" active centers, where active centers were removed by the formation of uniform thin copper film by electrodeposition at some lower overpotential [18].

4.2.2.3 Concentration of Cu(II) Ions

The increase of concentration of Cu(II) ions causes a sharp decrease of the quantity of evolved hydrogen and hence the decrease of the average current efficiencies for hydrogen evolution reaction [19, 20], what is in a good agreement with the prediction of the ionic equilibrium of the species in the $CuSO_4$–H_2SO_4–H_2O system [21, 25, 26]. Electrodeposition processes from copper solutions containing the concentration of Cu(II) ions above 0.15 M $CuSO_4$ (in 0.50 M H_2SO_4) lead to the formation of new type of holes, denoted as dish-like hole [19]. The typical dish-like holes obtained by electrodeposition from 0.60 M $CuSO_4$ in 0.50 M H_2SO_4 at an overpotential of 1,000 mV are shown in Fig. 4.5a. The appearance of very branchy dendrites between dish-like holes (Fig. 4.5b), and at shoulders of holes with longer electrodeposition times (Fig. 4.5c) clearly points out that the diffusion layer of the macroelectrode is not disturbed during copper electrodeposition from this solution, and that the quantity of evolved hydrogen

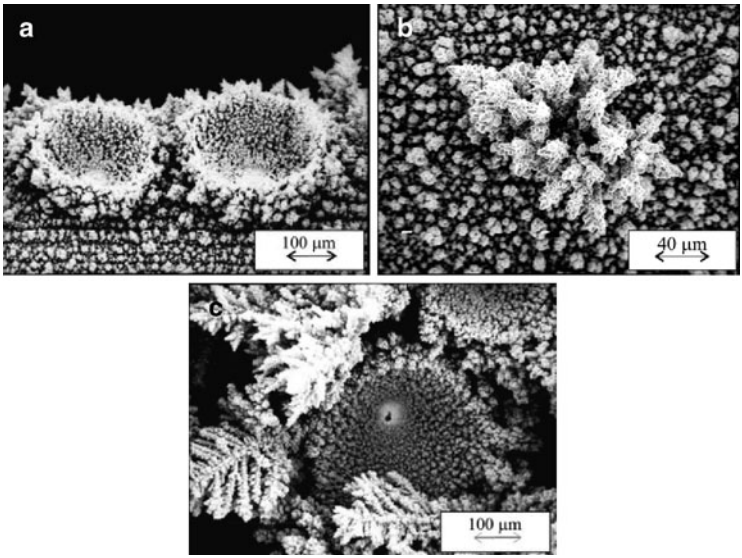

Fig. 4.5 Copper deposits electrodeposited from 0.60 M $CuSO_4$ in 0.50 M H_2SO_4 at an overpotential of 1,000 mV. Quantity of electricity: (**a**) and (**b**) 2.5 mAh/cm^2 and (**c**) 20 mAh/cm^2 (Reprinted from [19] with permission from Elsevier and [23] with permission from Springer.)

was not enough to cause stirring of solution in the near-electrode layer. Honeycomb-like structures were formed during copper electrodeposition from solutions with concentrations of Cu(II) ions less than 0.15 M $CuSO_4$ (for example, from 0.075 M $CuSO_4$ in 0.50 M H_2SO_4) [19].

The concentration of 0.30 M $CuSO_4$ (in 0.50 M H_2SO_4) is the transitional concentration between lower and higher concentrations of Cu(II) ions. The mixture of holes forming the honeycomb-like structure and dish-like holes was obtained by electrodeposition from this solution at an overpotential of 1,000 mV (Fig. 4.6) [19].

4.2.2.4 Concentration of Sulfuric Acid

The effect of H_2SO_4 on copper electrodeposition processes was examined keeping the concentration of Cu(II) ions constant

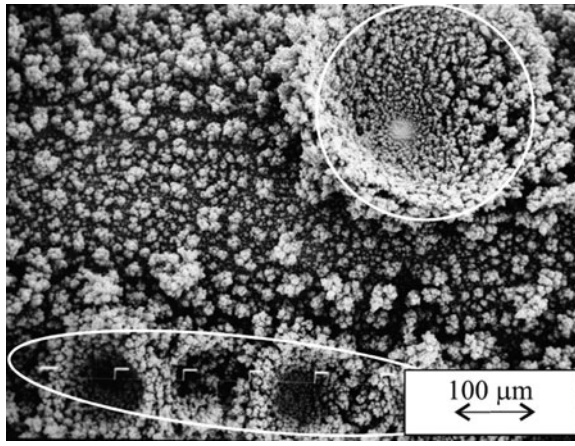

Fig. 4.6 Copper deposit obtained at an overpotential of 1,000 mV from 0.30 M $CuSO_4$ in 0.50 M H_2SO_4 with a quantity of the electricity of 2.5 mAh/cm^2 (Reprinted from [19] with permission from Elsevier and [23] with permission from Springer.)

(0.15 M $CuSO_4$), while the concentration of H_2SO_4 was varied, and they were 0.125, 0.25, and 1.0 M H_2SO_4 [22]. As expected, the increasing H_2SO_4 concentration led to the increase of the average current efficiencies of hydrogen evolution. The main characteristics of electrodeposition processes at an overpotential of 1,000 mV from the solutions containing 0.15 M $CuSO_4$ in both 0.25 and 1.0 M H_2SO_4 were holes or pores surrounded by agglomerates of copper grains. Aside from holes and cauliflower-like agglomerates of copper grains between them, degenerate dendrites, a channel structure around dendritic and cauliflower-like particles and holes with the shoulders of degenerate dendrites were electrodeposited at 1,000 mV from 0.15 M $CuSO_4$ in 0.125 M H_2SO_4 [22, 23]. These morphological forms were obtained in spite of relatively high average current efficiency of hydrogen evolution of 20.3% by which this deposit was formed, and their formation can be explained by the effect of a density and a surface tension of the electroplating solution on the bubble break-off diameter [22, 23]. The number of holes increased with the increasing H_2SO_4 concentration, while the hole size decreased with the increasing H_2SO_4 concentration. Also, the

orientation of holes was changed from random oriented holes to holes which were lined up in parallel rows [22].

4.2.2.5 Temperature of Electrolysis

The increase of temperature of electrolysis leads to an intensification of hydrogen evolution reaction [27]. Meanwhile, despite intensification of hydrogen evolution with the increasing temperature, the decrease of the number of holes formed per mm^2 surface area of electrodes and the increase of their average diameter were observed during copper electrodeposition at an overpotential of 800 mV (Fig. 4.7). To explain this unexpected trend in the development of morphology of electrodeposited copper, the effect of temperature on some properties of electroplating solution, such as viscosity and surface tension, is considered [27]. The increase of temperature causes the decrease of both the viscosity [28] and the surface tension of this solution [29]. The decrease of the surface tension of the solution lowers the break-off diameter of the hydrogen bubble from the electrode surface [29], while the decreased viscosity of the solution probably facilitates a transport of the detached hydrogen bubbles through the interior of the deposit forming the channel structure through it. Anyway, increasing temperature leads to redistribution of evolved hydrogen from those creating honeycomb-like structure (Fig. 4.7a, b) to structure with dish-like holes (Fig. 4.7c) and by the dominant presence of agglomerates of copper grains surrounded by irregular channels of evolved hydrogen (that is a channel structure) (Fig. 4.7d).

4.2.2.6 Time of Electrolysis

The size of holes increases with electrolysis time due to the growth of the hydrogen bubbles with time, as well as due to a coalescence of neighboring hydrogen bubbles. In the growth process, due to the current density distribution effect, some hydrogen bubbles can remain captive in the interior of deposit making the honeycomb-like structure very porous (Fig. 4.8; part in circle denoted with *D*) [24].

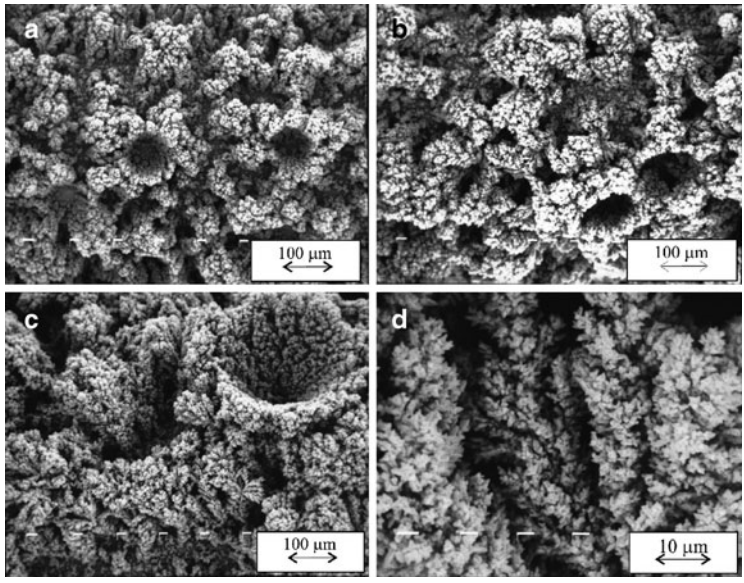

Fig. 4.7 Copper deposits electrodeposited at an overpotential of 800 mV from 0.15 M $CuSO_4$ in 0.50 M H_2SO_4 at temperatures of: (**a**) 14.0; (**b**) 35.0; (**c**) and (**d**) 50.0 ± 0.5°C. Quantity of electricity: 10 mAh/cm^2 (Reprinted from [27] with permission from Serbian Chemical Society and [23] with permission from Springer.)

4.3 Galvanostatic Regime of Electrolysis

In galvanostatic regimes of electrolysis, the honeycomb-like structures are formed at current densities larger than the limiting diffusion current density [30]. The typical honeycomb-like structure electrodeposited at a current density of 0.44 A/cm^2, which is about 27.5 larger than the limiting diffusion current density, is shown in Fig. 4.9a. From Fig. 4.9b–d, all elements of which this structure type is constructed can be seen: individual hole formed by attached hydrogen bubble (this type of hole is denoted as noncoalesced hole in the future text; Fig. 4.9b), hole formed by coalescence of closely formed hydrogen bubbles (this type of hole is denoted as coalesced

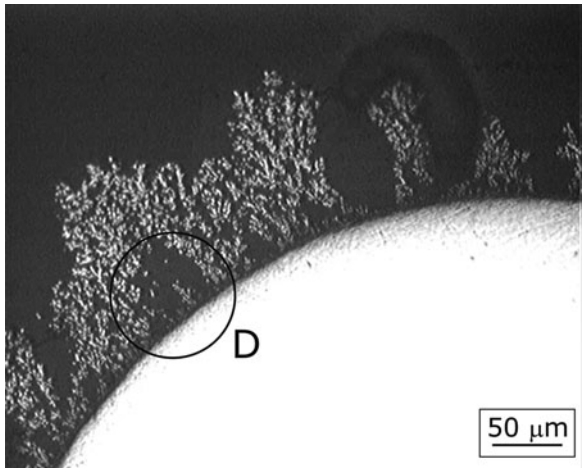

Fig. 4.8 Cross section of copper deposit electrodeposited from 0.15 M $CuSO_4$ in 0.50 M H_2SO_4 at an overpotential of 1,000 mV with a quantity of the electricity of 10 mAh/cm^2 (Reprinted from [24] with permission from Serbian Chemical Society.)

hole in the future text; Fig. 4.9c), and cauliflower-like agglomerates of copper grains formed around holes (Fig. 4.9d).

The hole size decreases while the number of holes increases with the increasing current density of electrodeposition [5].

4.4 A Brief Review of Previous Results

The increasing overpotential, the decreasing concentration of Cu(II) ions, and the increasing H_2SO_4 concentration intensify the hydrogen evolution reaction. The intensification of hydrogen evolution leads to an increase of the number of formed holes, as well as to a decrease of hole size. Meanwhile, the ratio of the coalesced holes to the overall number of formed holes increased with the intensification of hydrogen evolution.

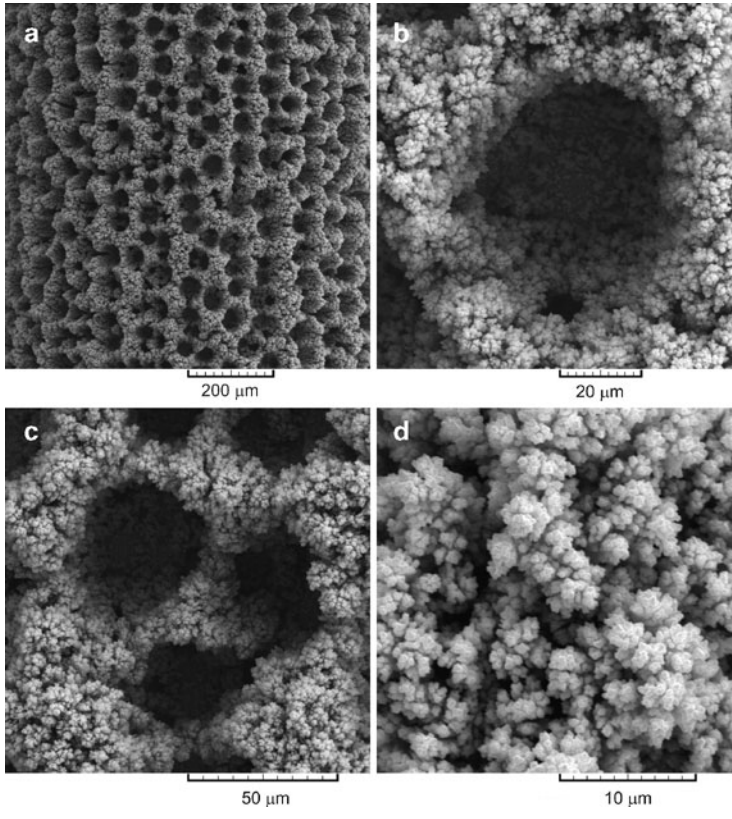

Fig. 4.9 (**a**) The honeycomb-like structure formed at a current density of 0.44 A/cm^2 and the typical elements constructing this type of structure; (**b**) noncoalesced hole; (**c**) coalesced hole; and (**d**) cauliflower-like agglomerates of copper grains formed around holes (Reprinted from [30] with permission from Elsevier.)

The process of a coalescence of closely formed hydrogen bubbles should be avoided during the formation of the honeycomb-like deposits because this process causes both the decrease of the overall number of the formed holes and the increase of the hole size and hence leads to the decrease of the specific surface area of these electrodes.

To increase the specific surface area and enhance the effectiveness/activity of the porous electrodes, it is necessary to reduce the size of the pores, as well as the branches in the foam or agglomerates of copper grains in the honeycomb-like structures [4].

The two ways are proposed to increase the specific surface area of open porous copper electrodes and to improve micro- and nanostructural characteristics of these electrodes. The first way is the addition of specific substances, known as additives, to the electroplating solution [4]. So, the decrease of the diameter of holes, as well as the increase of their number in 3D foam copper structures, can be realized by the addition of acetic acid to the copper sulfate solution [4]. Also, the addition of chloride ions dramatically reduces the size of the copper branches in the walls of holes. The reduction in pore size is a result of lowering hydrophobic force of the generated hydrogen gas by adding bubble stabilizer (e.g., acetic acid) that suppresses the coalescence of bubbles, while the decrease in branch size in the foam wall is a consequence of the catalytic effect of chloride ions on the copper deposition reaction. Mechanical strength of the foam structure can be improved by the addition of $(NH_4)^+$, Cl^-, polyethylene glycol, and 3-mercapto-1-propane sulfonic acid to the deposition bath [31]. The foam structure obtained by a combination of these additives was a highly porous with better mechanical strength than the one obtained without additives, owing to higher compactness of crystallites. Meanwhile, the use of additives in electroplating practice leads to their consumption during electrodeposition processes and the requirement for their permanent control is necessary. The consumption of additives occurs due to removal with the plated objects, by their incorporation in the deposit (codeposition) and by reaction on the plated object [32, 33].

The second way for the increase of the specific surface area of copper electrodes is the application of periodically changing regimes of electrolysis, such as pulsating overpotential (PO), pulsating current (PC), and reversing current (RC). The application of PO regime is primarily important from academic point of view for understanding mechanism of electrodeposition processes at periodically changing rate. For technological purposes, pulse and reverse plating techniques, such as pulsating current (PC) and reversing current (RC), are more important [34, 35].

4.5 The Regime of Pulsating Overpotential

Pulsating overpotential (PO) consists of a periodic repetition of overpotential pulses of different shapes [34, 35]. Square-wave PO is defined by the overpotential amplitude, η_A, deposition pulse, t_c, and pause, t_p. The pause to pulse ratio is defined as $p = t_p/t_c$.

4.5.1 Characteristics of the Honeycomb-Like Structures Obtained by the PO Regime and Their Comparison with Those Obtained by the Constant Regimes of Electrolysis

Figure 4.10 shows the honeycomb-like electrodes obtained at a constant overpotential of 1,000 mV (Fig. 4.10a) and by the PO regime with the overpotential amplitude of 1,000 mV, deposition pulse, t_c, of 10 ms, and pause duration, t_p, of 50 ms (Fig. 4.10b). The difference in the number of holes, as well as in their size, can be clearly seen from this figure. In all experiments for which results are presented in this section,

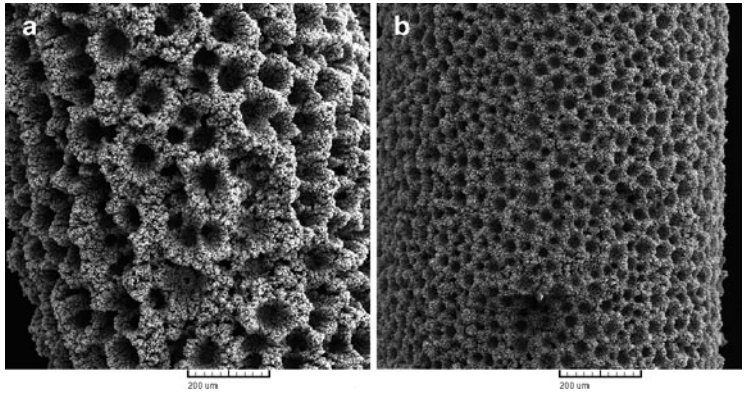

Fig. 4.10 Honeycomb-like structures obtained: (**a**) at a constant overpotential of 1,000 mV and (**b**) by PO regime with deposition pulse of 10 ms and a pause of 50 ms (Reprinted from [36] with permission from Elsevier.)

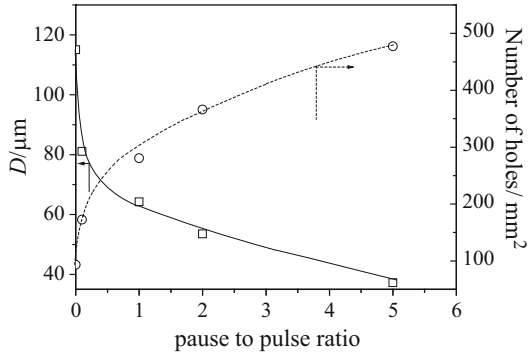

Fig. 4.11 The dependences of the average diameter of the surface holes, *D*, (*square*) and the number of holes per mm^2 surface area of the copper electrode (*circle*) on the pause to pulse ratio (Reprinted from [36] with permission from Elsevier.)

electrodeposition of copper was performed from 0.15 M $CuSO_4$ in 0.50 M H_2SO_4 at room temperature using cylindrical copper electrodes [24, 36, 37]. In pulsating overpotential (PO) deposition the overpotential amplitude of 1,000 mV and pulse duration of 10 ms were applied. A pause duration was selected to be 5, 10, 20, 50, and 100 ms (the pause to pulse ratios were 0.5, 1, 2, 5, and 10, respectively).

The dependences of the average diameter of the holes and of the number of holes formed per mm^2 surface area of the honeycomb-like copper electrodes on the pause to pulse ratio are shown in Fig. 4.11.

The decrease of the hole size and the increase of the number of formed holes with the increasing pause to pulse ratio can be primarily ascribed to the suppression of a coalescence of closely formed hydrogen bubbles [36]. The coalesced holes are observed in the honeycomb-like structures formed with pause to pulse ratios up to 2. Holes formed with the pause durations shorter than the deposition pulse were similar to those obtained at constant overpotential [36]. The bottom of these holes was very compact (Fig. 4.12a, b). The prolonging pause duration led to the change of the bottom of holes from compact to the one constructed of very disperse agglomerates of copper grains (Fig. 4.12c). The significantly smaller number of holes was formed with a pause duration of 100 ms and

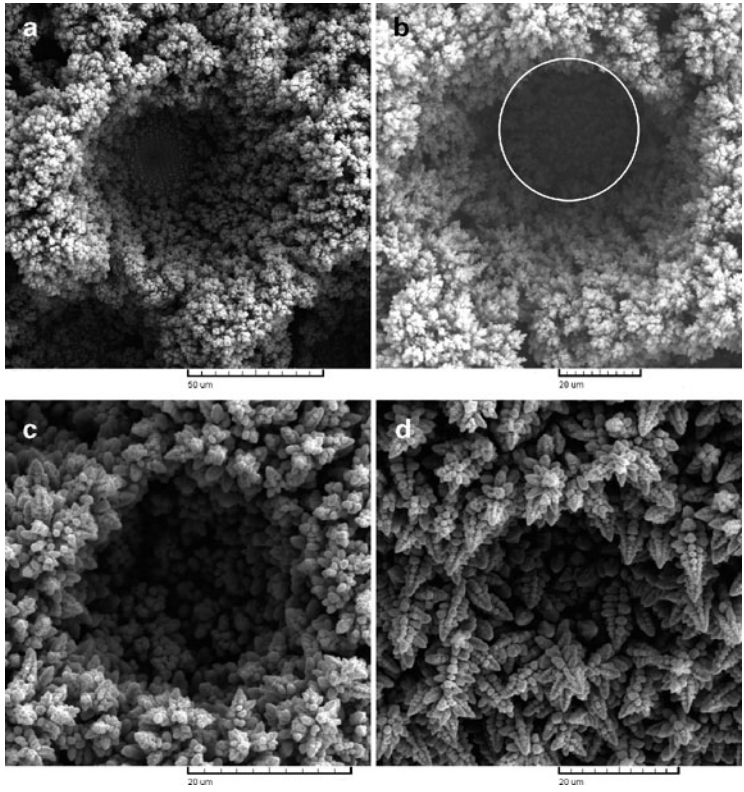

Fig. 4.12 Holes formed by attached hydrogen bubbles obtained at: (**a**) a constant overpotential of 1,000 mV and by PO regimes with a pause duration of: (**b**) 5 ms; (**c**) 50 ms; and (**d**) 100 ms. Deposition pulse: 10 ms (Reprinted from [36] with permission from Elsevier and [37] with permission from Springer.)

these holes were completely different from those obtained with the smaller pause to pulse ratios [37]. This type of holes was constructed from dendrites (Fig. 4.12d).

Simultaneously, the morphology of electrodeposited copper formed around holes, as well as inside holes, changed with the increasing pause to pulse ratio from cauliflower-like agglomerates of copper grains to dendrites. Very disperse agglomerates of copper grains were formed at the constant overpotential and by the PO

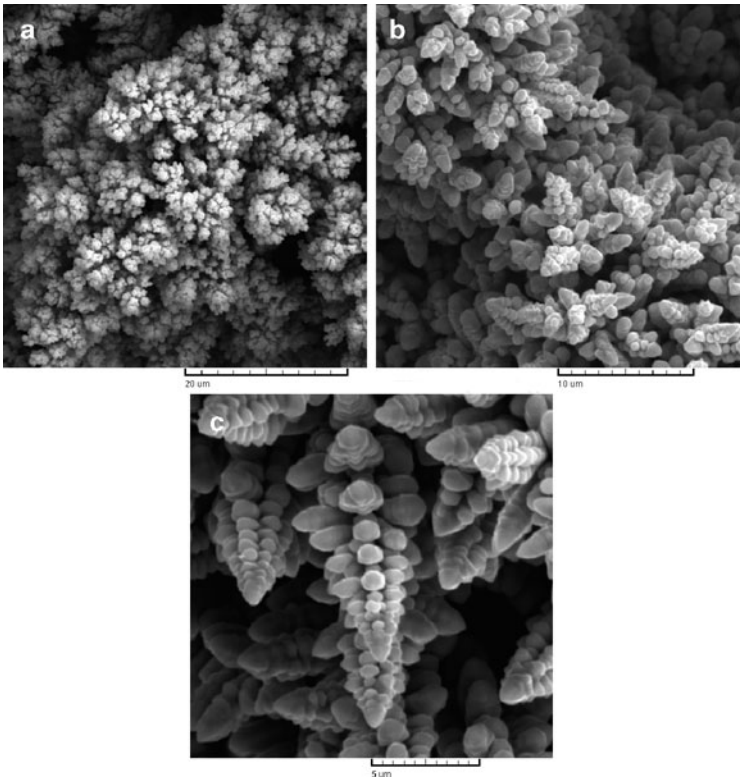

Fig. 4.13 Morphologies of electrodeposited copper formed around holes: (**a**) at a constant overpotential of 1,000 mV and by the PO regimes with pause duration of: (**b**) 50 ms and (**c**) 100 ms. Deposition pulse: 10 ms (Reprinted from [36, 38] with permission from Elsevier.)

regimes with pause durations shorter than the deposition pulse (Fig. 4.13a). Copper dendrites are noticed at shoulders of holes electrodeposited with pause duration of 20 ms and their number and size increased with the prolonging pause durations, as shown in Fig. 4.13b for the morphology of electrodeposited copper obtained with a pause duration of 50 ms. Finally, the walls of holes obtained with pause duration of 100 ms were only composed of dendrites (Fig. 4.13c). The appearing of dendritic forms clearly

indicates a decrease of effectiveness of stirring of copper solution by evolved hydrogen with the increase of pause duration.

The analysis of the interior of holes obtained with pause durations up to 50 ms showed that the prolongation of pause duration leads to a reduction of the size of agglomerates of copper grains of which the walls of holes are constructed. With the prolonging pause duration up to 50 ms, holes became closer to each other, while compactness of the formed agglomerates between them was also increased [36]. The size of grains of which both cauliflower-like agglomerates and dendrites are composed increased with increasing pause to pulse ratio due to the selective dissolution of grains during the pauses. It was shown [39] that the smaller grains would dissolve faster than the larger ones due to the Kelvin effect [40]. In addition, the structure of the grains becomes more regular with increasing pause duration due to the fact that the adatoms in nonstable positions dissolve faster than the atoms in a stable position in lattice [35]. Finally, the deposit at the shoulders of the holes dissolve faster due to the edge effect, which also leads to the formation of a more homogenous distributed deposit with increasing pause duration and to an increased number of less deep holes.

The increased compactness of the copper deposits, the suppression of coalescence of neighboring hydrogen bubbles, and a decrease of the depth of the holes can be clearly seen from Fig. 4.14 showing cross section of copper deposits obtained with different pause to pulse ratios [24]. The compactness of the formed deposits increased with the increasing pause duration [24], and it was larger than the compactness of the deposit obtained by the constant regime of electrolysis (Fig. 4.4a). From Figs. 4.8 and 4.14, it can be seen that the increase of the number of holes by the application of PO regime can be ascribed not only to supressed coalescence of neighboring hydrogen bubbles but also to the improved current distribution at growing copper surface by which an inclusion of hydrogen bubbles in deposit was prevented. Due to the current density distribution effect, the loosing of "irregular holes" was also observed by the application of PO regimes. With the prolonging pause duration, pores or channels formed through the interior of deposits were mutually coalesced forming larger pores. In this way, a transport of electroactive species through the interior of structures was facilitated, what is very desirable for evaluation of electrochemical reactions [1].

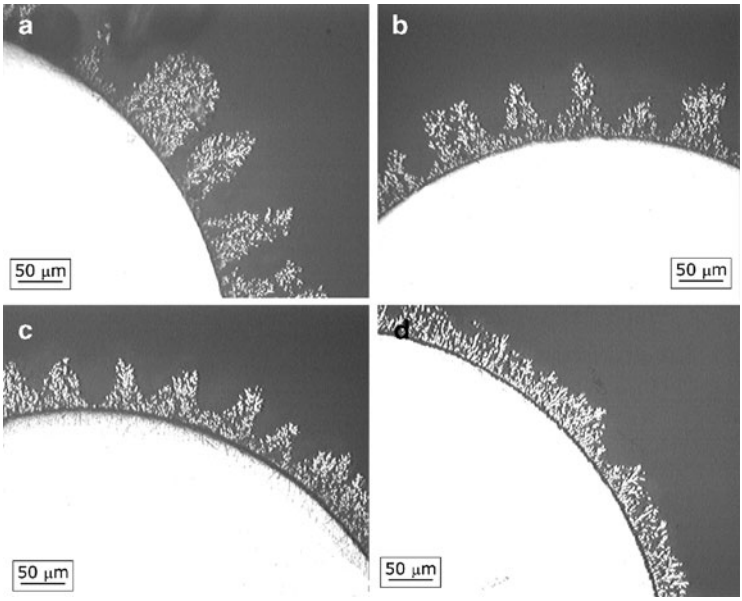

Fig. 4.14 Cross section of copper deposits electrodeposited by pulsating overpotential (PO) regime with pause duration of: (**a**) 5 ms; (**b**) 20 ms; (**c**) 50 ms; and (**d**) 100 ms. Deposition pulse: 10 ms (Reprinted from [24] with permission from Serbian Chemical Society.)

Anyway, the effects observed by the application of PO regime are ascribed to a current density during "off" periods (i.e., during duration of pause). Although this current density can be neglected in comparison with the current density during "on" periods (i.e., during the duration of deposition pulse), it is clear that its effect on the formation of these deposits is very important [36, 37].

4.5.2 Formation of the Honeycomb-Like Structures by the PO Regime

The values of the average current efficiencies of hydrogen evolution, $\eta_{I,av}(H_2)$, obtained for different pause to pulse ratios are given in Table 4.1 [41]. The following parameters of square-waves PO were

Table 4.1 The values of the average current efficiencies of hydrogen evolution, $\eta_{I,av}(H_2)$, in %, obtained for different pause to pulse ratios (t_c deposition pulse; t_p pause duration)

t_c:t_p	1:10	3:10	5:10	10:10	20:10
$\eta_{I,av}(H_2)$ (%)	0	16.4	22.4	27.2	28.1

Reprinted from [41] with permission from Elsevier

analyzed: the overpotential amplitude of 1,000 mV, pause duration of 10 ms, and deposition pulses of 1, 3, 5, 10, and 20 ms.

The pyramid-like forms were electrodeposited by square-wave PO with a deposition pulse of 1 ms (Fig. 4.15a, b). These pyramid-like forms represent precursors of dendrites, what is concluded by the comparison with the top of copper dendrites obtained by copper electrodeposition at a constant overpotential of 650 mV (Fig. 4.15c). Copper pyramids of different shapes are also obtained by electrodeposition in a constant regime of electrolysis, where the morphology of pyramidal nanoparticles depended on the ratio of the concentration of surfactant/precursor and deposition time [42]. Despite the fact that the overpotential amplitude of 1,000 mV was used, holes for which the origin was of attached hydrogen bubbles were not formed (Fig. 4.15a). The absence of holes clearly indicates that a deposition pulse of 1 ms was insufficient for the formation of hydrogen bubbles.

From Fig. 4.16, it can be seen that honeycomb-like structures were formed with deposition pulses of 3, 5, 10, and 20 ms. The analysis of the honeycomb-like structures showed that the number of holes formed by the attached hydrogen bubbles did not change considerably with the length of deposition pulses of 3, 5, and 10 ms (i.e., with pause to pulse ratios up to 1). The mild decrease of the number of the formed holes was observed with a deposition pulse of 20 ms, what can be ascribed to the enhanced coalescence of neighboring hydrogen bubbles as well as to effects related to the current density distribution at the growing electrode by which some of the hydrogen bubbles remained captive in the interior of deposits [41].

Meanwhile, the strong effect of the length of deposition pulse on the morphology of electrodeposited copper formed around holes was achieved (Fig. 4.17). Copper dendrites were formed with a deposition

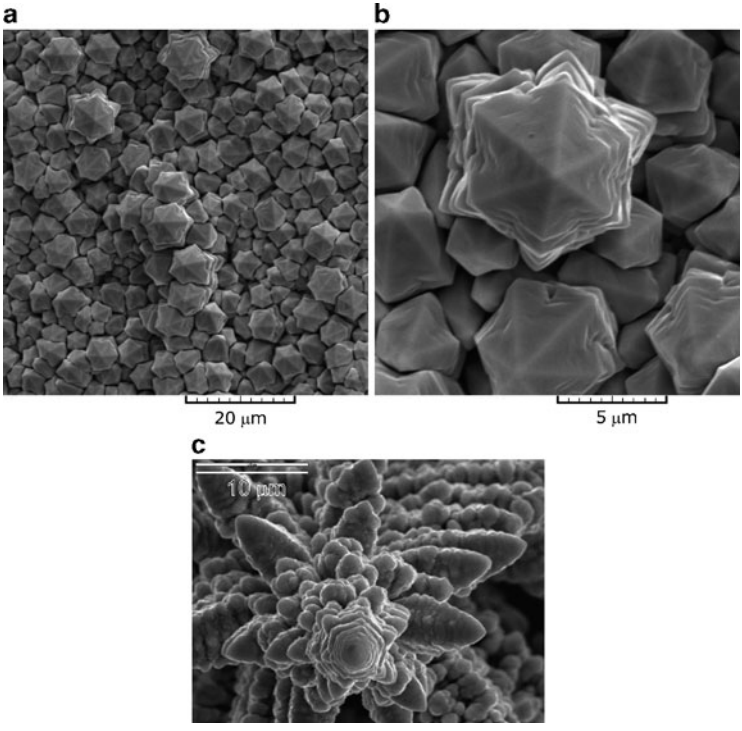

Fig. 4.15 (**a**) and (**b**) Pyramid-like precursors of dendrites obtained by square-wave PO with a deposition pulse of 1 ms and a pause of 10 ms; deposition time: 1,800 s, (**c**) top view of copper dendrite obtained by electrodeposition at an overpotential of 650 mV (Reprinted from [41] with permission from Elsevier.)

pulse of 3 ms (Fig. 4.17a). Although dendrites were also formed with a deposition pulse of 5 ms (Fig. 4.17b), there were more branchy structures than those obtained with a deposition pulse of 3 ms (Fig. 4.17a). Agglomerates of copper grains were mainly formed with a deposition pulse of 10 ms, while the presence of developed dendrites was very rare (Fig. 4.17c). Finally, agglomerates of copper grains were formed between holes when deposition pulse of 20 ms was applied (Fig. 4.17d).

Figure 4.18 shows the cross section of the copper deposits obtained with deposition pulses of 3, 5, 10, and 20 ms. Dendrites formed around

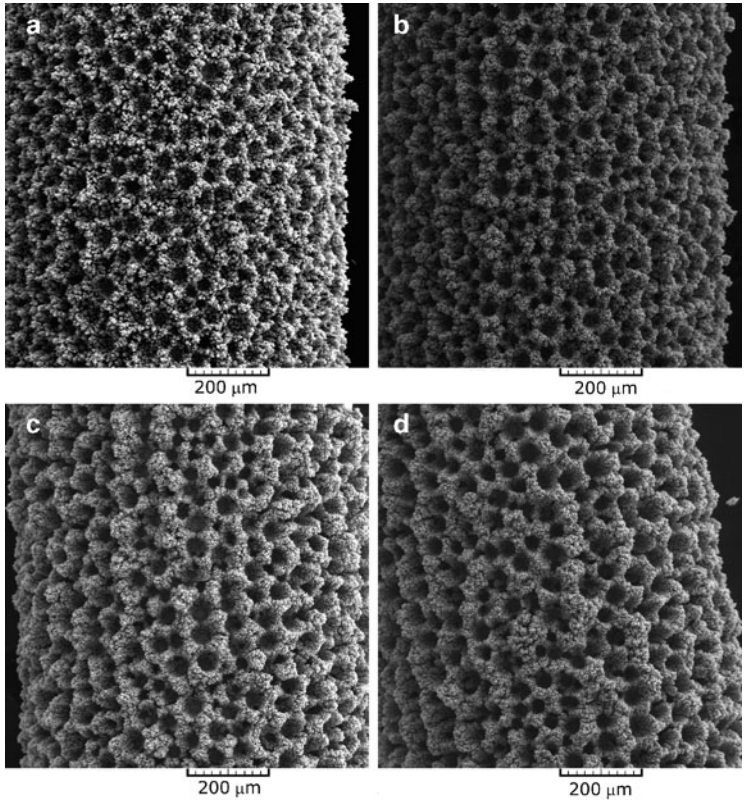

Fig. 4.16 Honeycomb-like copper structures obtained by the PO regimes with deposition pulses of: (**a**) 3 ms; (**b**) 5 ms; (**c**) 10 ms; and (**d**) 20 ms. Pause duration: 10 ms (Reprinted from [41] with permission from Elsevier.)

the hydrogen bubbles in the copper deposit obtained with a deposition pulse of 3 ms are clearly seen from Fig. 4.18a. The analysis of Fig. 4.18b confirmed that more branchy dendrites are formed with a deposition pulse of 5 ms than with 3 ms. Further increase of the deposition pulse led to the increase of a dispersity of the internal structures of the copper deposits, which is observed from Fig. 4.18c, d showing the cross sections of the copper deposits obtained with deposition pulses of 10 and 20 ms. The numbered channels formed

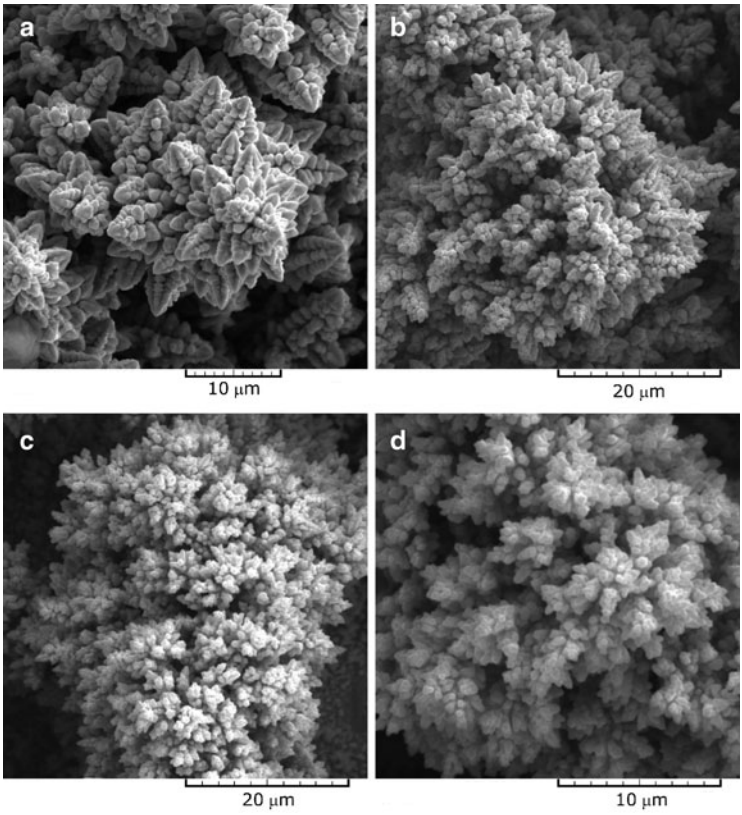

Fig. 4.17 Morphology of electrodeposited copper formed around holes by the PO regimes with deposition pulses of: (**a**) 3 ms; (**b**) 5 ms; (**c**) 10 ms; and (**d**) 20 ms. Pause duration: 10 ms (Reprinted from [41] with permission from Elsevier.)

around relatively small copper particles and degenerate dendrites are easily observed from Fig. 4.18c, d. From Fig. 4.18, it can also be seen that the depth of holes did not change noticeably when deposition pulses of 3, 5, and 10 ms were applied. The depth of the hole obtained with a deposition pulse of 20 ms was larger than those obtained with 3, 5, and 10 ms, what can be ascribed to the enhanced dispersity of this deposit. The analysis of holes shown in Fig. 4.18 showed that there

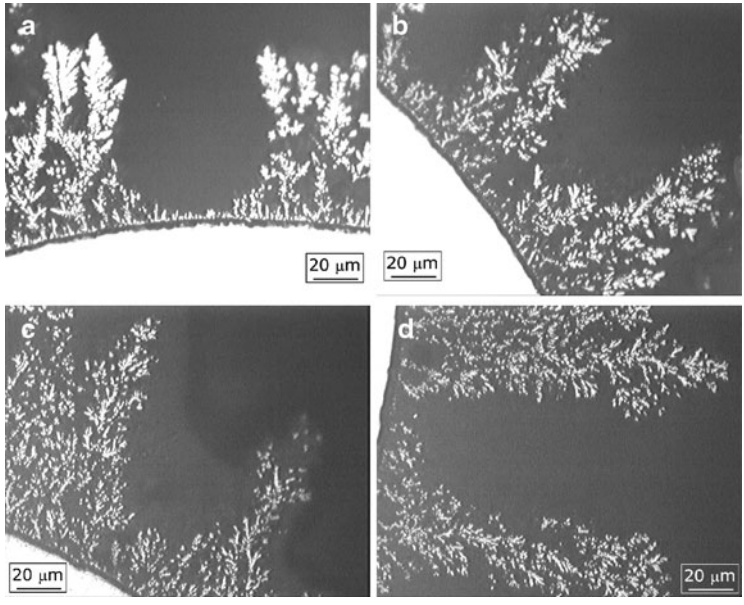

Fig. 4.18 Cross section of the copper deposits obtained with deposition pulses of: (**a**) 3 ms; (**b**) 5 ms; (**c**) 10 ms; and (**d**) 20 ms. Pause duration: 10 ms (Reprinted from [41] with permission from Elsevier.)

was not any effect of deposition pulse duration on the size of holes. The average diameter of holes obtained with deposition pulses of 3, 5, 10, and 20 ms (for pause duration of 10 ms) was estimated to be 65 ± 2.0 μm [41].

Then, the formation of the honeycomb-like structures by the PO regimes, as well as the change of morphology of the electrodeposited copper from dendrites to degenerate dendrites and cauliflower-like agglomerates of copper grains, can be explained as follows: similar to the constant regimes of electrolysis, in the initial stage of the electrodeposition process, both the nuclei of copper and the "nuclei" of the hydrogen bubbles are formed at the active sites of the electrode surface [18]. The number of the formed hydrogen bubbles is determined by the overpotential amplitude. Since the formed bubbles isolate electrode surface, electrodeposition of copper occurs around

them forming rings consisted of agglomerates of copper grains. In the growth process, during deposition pulse, due to a concentration of current lines, both copper nucleation and hydrogen evolution primarily occur at these agglomerates of copper grains. Some of the new, freshly formed hydrogen bubbles coalesce with the hydrogen bubbles formed in the initial stage, leading to their growth with electrolysis time.

Meanwhile, some of the freshly formed hydrogen bubbles cannot find a path to coalesce with them, and these hydrogen bubbles start to grow independently making an interior of deposit to be porous. Due to a constant value of pause duration of 10 ms, the effect of pause duration was the same for all deposition pulses. During the pause, the dissolution of both copper particles and the formed hydrogen bubbles occur.

The prolonging duration of deposition pulse increases both copper deposition and hydrogen evolution rates. This means a greater number of both new hydrogen bubbles and copper "nuclei" is formed with the prolonging deposition pulses. The greater part of these freshly formed bubbles will not find a path to coalesce with the previously formed hydrogen bubbles, because they are surrounded by freshly formed copper grains. Also, they will not be able to develop into large hydrogen bubbles the same reason. Due to impossibility for their further growth, these hydrogen bubbles will detach very fast from a growing electrode surface forming a channel structure through the interior of deposit and causing stirring of solution in the near-electrode layer.

The analysis of Figs. 4.15–4.18 confirms that the effectiveness of a stirring of solution increased with the increasing duration of deposition pulse. Because of the increased effectiveness of a stirring of solution by evolved hydrogen, the change of morphology of the electrodeposited copper from dendrites to degenerate dendrites and cauliflower-like agglomerates was observed.

On the basis of the same hole sizes and their unchanged number, as well as of the same depth of holes (Figs. 4.16–4.18), it can be concluded that the critical size of the hydrogen bubbles formed in the initial stage of electrodeposition process to be detached from electrode surface does not depend on the length of deposition pulse. It can be assumed that approximately a same quantity of evolved

hydrogen is used for the formation of these holes. Then, the difference between this quantity and the overall quantity of evolved hydrogen is responsible for a stirring of solution and a change of hydrodynamic conditions in the near-electrode layer. Also, it is clear that the quality of deposits formed between holes is determined by this difference in the quantity of evolved hydrogen.

4.5.3 *Energy Aspects of the Formation of the Honeycomb-Like Structures by the PO Regime*

Energy aspects of the formation of these electrodes can be obtained by the analysis of the specific energy consumption, w, which can be an important energy parameter in the development of these electrodes for commercial purposes. For electrodeposition process in PO regime, the specific energy consumption can be presented by Eq. (4.1) [41]:

$$w = \frac{nF\eta_A}{M(1 - \eta_{I,av}(H_2))}, \tag{4.1}$$

where η_A is the amplitude of overpotential, M is the molar mass of copper (63,55 g/mol), and the number of Faraday per mole of consumed ions of copper is 2×26.8 Ah/mol $= 53.6$ Ah/mol. Using the overpotential amplitude of 1,000 mV, and the values of $\eta_{I,av}(H_2)$ obtained with deposition pulses of 3 and 10 ms (Table 4.1), it can be shown that the shortening of deposition pulse from 10 to 3 ms leads to the decrease of the specific energy consumption for about 15%. Simultaneously, the number, diameter, and depth of holes remained unchanged. Considering the unchanged number of holes with the approximate same diameter and depth, it is clear that the use of shorter deposition pulses showed as a valuable way for energy saving in a production of this structure type.

Aside from energy savings attained by the application of PO regime, the improvement of mechanical strength of the honeycomb-like

structures was noticed in the process of development of these deposits as possible electrodes. It can be assumed that the increase of mechanical strength is related to the decrease of the quantity of evolved hydrogen needed for their formation.

4.6 The Regime of Pulsating Current

The regime of pulsating current (PC) consists of a periodic repetition of square pulses [34, 35], and it is characterized by the amplitude of the cathodic current density, j_A, the deposition pulse, t_c (on period), and the pause duration, t_p, in which the system relaxes (off period). The average current density, j_{av}, is given by Eq. (4.2):

$$j_{av} = \frac{j_A t_c}{t_c + t_p} \tag{4.2}$$

or

$$j_{av} = \frac{j_A}{1 + p}, \tag{4.3}$$

if

$$p = \frac{t_p}{t_c}, \tag{4.4}$$

where p is the pause to pulse ratio.

In the PC regimes, the surface concentration of depositing ions is only determined by the average current density [34]. Then, the overpotential amplitude, η_A, can be presented by Eq. (4.5) [43]:

$$\eta_A = \frac{b_c}{2.3} \ln \frac{j_{av}(p+1)}{j_0} + \frac{b_c}{2.3} \ln \frac{1}{1 - \frac{j_{av}}{j_L}}, \tag{4.5}$$

where b_c is the cathodic Tafel slope, j_L is the limiting diffusion current density, and j_0 is the exchange current density. The activation part of overpotential, η_{act}, is

$$\eta_{\text{act}} = \frac{b_c}{2.3} \ln \frac{j_{\text{av}}}{j_0} (p+1) \tag{4.6}$$

while the diffusion part of overpotential, η_{diff}, is

$$\eta_{\text{diff}} = \frac{b_c}{2.3} \ln \frac{1}{1 - \frac{j_{\text{av}}}{j_L}}. \tag{4.7}$$

Equation (4.5) can be rewritten in the form

$$\eta_A = \eta_{\text{const}} + \frac{b_c}{2.3} \ln(p+1), \tag{4.8}$$

where η_{const} is the overpotential in the constant regime of electrolysis defined by Eq. (4.9):

$$\eta_{\text{const}} = \frac{b_c}{2.3} \ln \frac{j_{\text{av}}}{j_0} + \frac{b_c}{2.3} \ln \frac{1}{1 - \frac{j_{\text{av}}}{j_L}}, \tag{4.9}$$

if $j_{\text{av}} = j$, where j is the current density in the constant regime of electrolysis.

Equation (4.5) is valid in the frequency range 10–100 Hz, where the frequency is sufficiently high to produce constant concentration on the surface and sufficiently low that the effect of DC capacity can be neglected. Hence, in the analyzed frequency range from 10 to 100 Hz, the surface concentration of depositing ions is constant and equal to the one in the constant regime at the current density corresponding to the average current density in the PC regime [34, 35]. From the point of view of the average current density, it means that there is not any difference between electrochemical deposition processes in the constant regimes and PC conditions. On the other hand, it is very clear from Eq. (4.5) that at the fixed value of the average current density the amplitude of overpotential depends on pause to pulse ratio, and it increases with the increasing pause to pulse ratio.

According to Popov and Pavlović [43], the degree of diffusion control of electrodeposition process, ω, is defined by Eq. (4.10):

$$\omega = \frac{\ln \frac{1}{1-\frac{j_{av}}{j_L}}}{\ln \frac{j_{av}}{j_0} + \ln(p+1) + \ln \frac{1}{1-\frac{j_{av}}{j_L}}}, \tag{4.10}$$

and it represents a contribution of diffusion overpotential to total cathode overpotential. Hence, due to the increase of activation part of overpotential with the increasing pause to pulse ratio, the degree of diffusion control will decrease with the increasing pause to pulse ratio, resulting in the possible change of texture of deposit. It is noteworthy that it is valid if $j_{av} < j_L$ in the mixed controlled deposition.

In the hydrogen codeposition range, the current efficiency for metal electrodeposition is less than 1, and then the effective average current density, $j_{av}*$, can be presented by Eq. (4.11):

$$j_{av}* = \frac{\eta_{I,av}(M) j_A}{1+p}, \tag{4.11}$$

where $\eta_{I,av}(M)$ is the average current efficiency for metal electrodeposition.

Since

$$\eta_{I,av}(M) + \eta_{I,av}(H_2) = 1, \tag{4.12}$$

Eq. (4.11) can be rewritten as

$$j_{av}* = \frac{[1-\eta_{I,av}(H_2)] j_A}{1+p}, \tag{4.13}$$

and, according to Eqs. (4.3) and (4.11),

$$\eta_{I,av}(H_2) = 1 - \frac{j_{av}*}{j_{av}}. \tag{4.14}$$

In the hydrogen codeposition range, if $j_{av}* > j_L$, the amplitude of overpotential is related to the hydrogen reduction, increasing with the

current density of hydrogen evolution [43]. Equation (4.5) is still valid [43], but it must be modified and adapted to the effect of hydrogen evolution on metal electrochemical deposition process. Then, the modified Eq. (4.5) can be presented by Eq. (4.15):

$$\eta_{\mathrm{A,\,eff}} = \frac{b_{\mathrm{c}}}{2.3} \ln \frac{j_{\mathrm{av}}*(p+1)}{j_0} + \frac{b_{\mathrm{c}}}{2.3} \ln \frac{1}{1 - \frac{j_{\mathrm{av}}*}{j_{\mathrm{L}}*}}, \tag{4.15}$$

where $\eta_{\mathrm{A,eff}}$ represents the effective overpotential amplitude and $j_{\mathrm{L}}*$ is the effective limiting diffusion current density which depends on the hydrodynamic conditions in the near-electrode layer caused by hydrogen evolution during electrodeposition process. Equation (4.15) is valid if the condition $j_{\mathrm{av}}*/j_{\mathrm{L}}* < 1$ is fulfilled. The effective average current density, $j_{\mathrm{av}}*$, can be calculated by the use of Eq. (4.13) if the value of the average current efficiency of hydrogen evolution is known. Meanwhile, the determination of $j_{\mathrm{L}}*$ when the change of hydrodynamic conditions in the near-electrode layer is caused by hydrogen evolution is not possible. For that reason, the analysis of morphologies of electrodeposited copper obtained in the hydrogen codeposition range showed an excellent tool for the estimation of the change of effectiveness of solution stirring by evolved hydrogen.

It is very clear from the above consideration that the quantities of evolved hydrogen and hence the morphologies of electrodeposited metal will depend strongly on the applied parameters of PC regimes, such as the amplitude of the current density, deposition pulse, and pause duration.

4.6.1 Formation of the Honeycomb-Like Structures by the PC Regime

In PC regimes, the intensification of hydrogen evolution reaction can be achieved by:

1. The increase of the current density amplitude and keeping durations of both the deposition pulse and pause constant

2. The prolonging of a deposition pulse duration and keeping both the current density amplitude and pause duration constant
3. The shortening of a pause duration and keeping both the current density amplitude and deposition pulse constant

Since the second and third ways are closely related, these two ways will be analyzed simultaneously.

4.6.1.1 The Effect of the Current Density Amplitude

Figure 4.19 shows SEM micrographs of copper deposits obtained with the current density amplitudes of 0.20 A/cm^2 (Fig. 4.19a) and of 0.44 A/cm^2 (Fig. 4.19b). In both cases, a deposition pulse of 1 ms and a pause duration of 10 ms were applied. In all experiments related to the analysis of the PC regimes, copper electrodeposition was performed from 0.15 M $CuSO_4$ in 0.50 M H_2SO_4 at room temperature using the vertical stationary cylindrical copper electrodes [30, 44, 45].

Very branchy dendrites, small cauliflower-like forms, and shallow holes formed from detached hydrogen bubbles are formed when the amplitude of current density of 0.20 A/cm^2 was applied (Fig. 4.19a). On the other hand, dish-like holes and small cauliflower-like agglomerates of copper grains were formed with a current density amplitude of 0.44 A/cm^2 (Fig. 4.19b). The formation of these morphological forms was accompanied by the quantity of evolved hydrogen which corresponded to the average current efficiency of hydrogen evolution, $\eta_{I,av}(H_2)$, of 5.5% with the applied current density amplitude, j_A, of 0.20 A/cm^2 [45], and 13.7% with j_A of 0.44 A/cm^2 [30].

4.6.1.2 The Effect of the Length of Deposition Pulse

The prolongation of a duration of deposition pulse leads to the formation of honeycomb-like structures with both the current density amplitudes applied [30, 45]. The formation of this structure type is analyzed applying the current density amplitude of 0.44 A/cm^2, deposition pulses of 1, 4, 7, 10, and 20 ms, and a pause duration of 10 ms [30]. The values of the average current efficiency of hydrogen evolution, $\eta_{I,av}(H_2)$, obtained for these parameters of PC regimes are

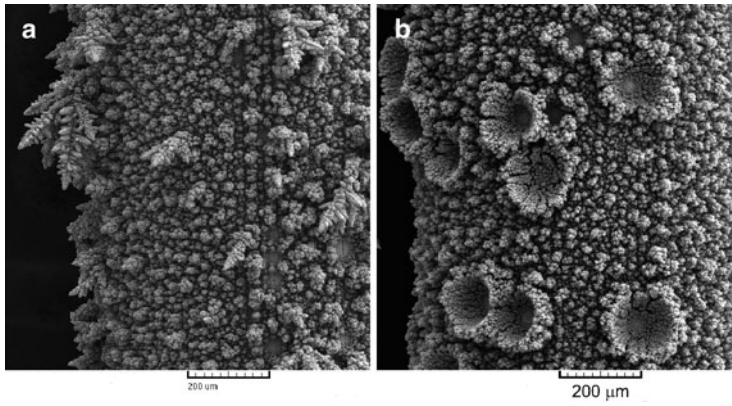

Fig. 4.19 Copper deposits obtained by the regime of pulsating current. The current density amplitude: (**a**) 0.20 A/cm^2 and (**b**) 0.44 A/cm^2. Deposition pulse: 1 ms. Pause duration: 10 ms (Reprinted from [30, 45] with permission from Elsevier.)

Table 4.2 The values of the average current efficiencies of hydrogen evolution, $\eta_{I,av}(H_2)$, in %, the average current efficiencies for copper electrodeposition, $\eta_{I,av}(Cu)$, in %, and the specific energy consumptions obtained for electrodeposition of copper with different pause to pulse ratios

t_c (ms)	1	4	7	10	20	Const. regime
$\eta_{I,av}(H_2)$ (%)	13.7	20.7	24.4	30.0	32.5	36.0
$\eta_{I,av}(Cu)$ (%)	86.3	79.3	75.6	70.0	67.5	64.0
w (kWh/kg)	1.075	1.170	1.228	1.326	1.375	1.450

Reprinted from [30] with permission from Elsevier
t_c deposition pulse in ms; t_p pause duration in ms ($t_p = 10$ ms); $j_A = 0.44$ A/cm^2

given in Table 4.2. Also, the value of $\eta_{I,av}(H_2)$ obtained for copper electrodeposition at the constant current density of 0.44 A/cm^2 is included in this table.

Using j_A of 0.44 A/cm^2, the honeycomb-like structures are formed with deposition pulses of 7 ms and longer and the typical honeycomb-like structure obtained with a deposition pulse of 10 ms is shown in Fig. 4.20a. The mixture of dish-like holes and holes constructing the honeycomb-like structure was formed with a deposition pulse of 4 ms (Fig. 4.20b). Finally, as already mentioned, dish-like holes and independently formed agglomerates of copper grains were formed with a deposition pulse of 1 ms (Fig. 4.19b).

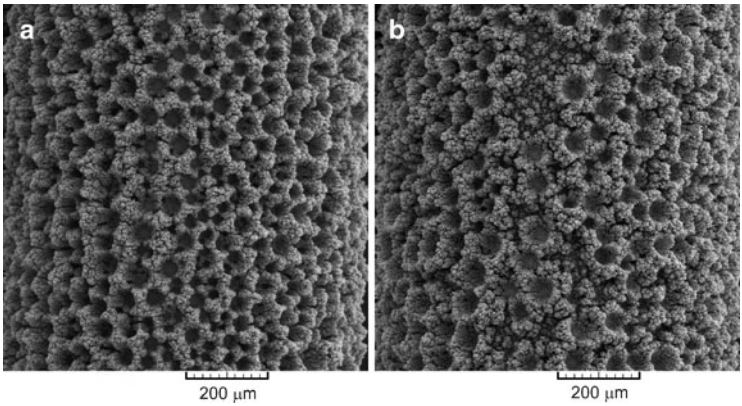

Fig. 4.20 Copper deposits obtained by the PC regimes with a deposition pulse of: (**a**) 10 ms and (**b**) 4 ms. Pause duration: 10 ms. The amplitude of current density: 0.44 A/cm^2 (Reprinted from [30] with permission from Elsevier.)

The shape, size, and number of holes strongly depended on the length of deposition pulse. The honeycomb-like structure electrodeposited with a deposition pulse of 20 ms was constructed of noncoalesced and coalesced holes (Fig. 4.21a, b, respectively). The decreasing length of deposition pulse led to the supression of the coalescence process. Noncoalesced holes formed with a deposition pulse of 10 ms were very similar to those obtained with a deposition pulse of 20 ms. Aside from the appearing of slightly larger holes than those formed with the deposition pulse of 10 ms, the decrease of deposition pulse to 7 ms did not have any effect on the shape and the size of holes. The mixture of dish-like holes and the noncoalesced holes constructing the honeycomb-like structure was formed with a deposition pulse of 4 ms [30]. The typical dish-like hole formed with a deposition pulse of 1 ms is shown in Fig. 4.21c.

Figure 4.22 shows the dependences of the average diameter of holes and the number of holes per mm^2 surface area of the copper electrode on pause to pulse ratio. In these dependences, the values obtained at the constant current density ($j = 0.44$ A/cm^2; $p = 0$) are also included. From Fig. 4.22 can be seen that the size of noncoalesced holes in the honeycomb-like structures did not depend on the length of deposition pulse. As expected, the size of dish-like

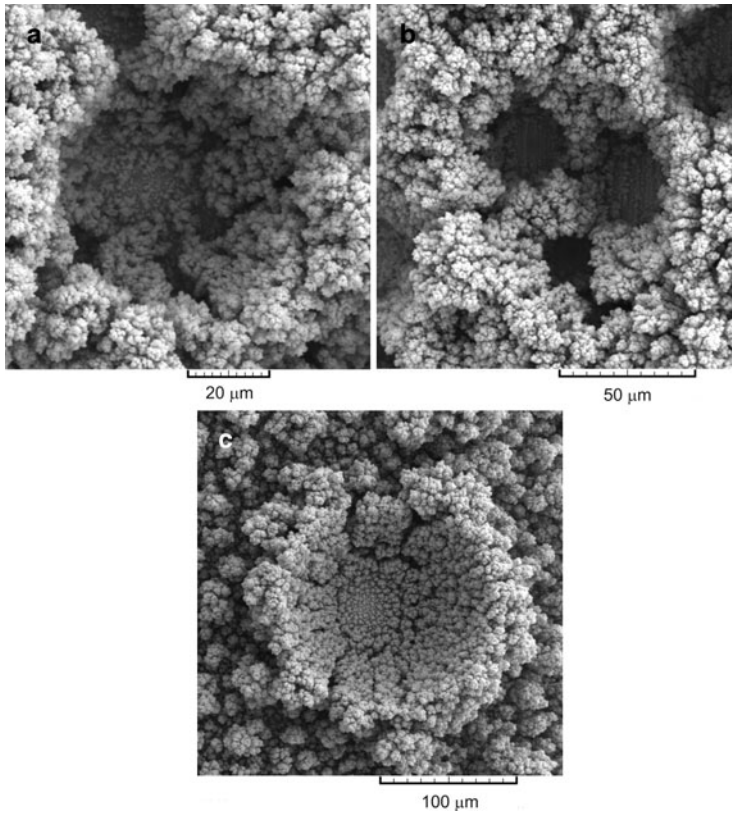

Fig. 4.21 The typical holes formed by the PC regimes with a deposition pulse of: (**a**) and (**b**) 20 ms; and (**c**) 1 ms. Pause duration: 10 ms. The amplitude of current density: 0.44 A/cm^2 (Reprinted from [30] with permission from Elsevier.)

holes was larger than those forming the honeycomb-like structures [19]. On the other hand, the dependence of the number of holes on the pause to pulse ratio shows maximal value for a pause to pulse ratio of 1 ($t_c = 10$ ms). The increase of number of holes obtained with a pause to pulse ratio of 0.5 ($t_c = 20$ ms) in relation to the one formed at the constant current density ($p = 0$) is due to the decreased coalescence of closely formed hydrogen bubbles. The maximum of the dependence obtained for a pause to pulse ratio of 1 ($t_c = 10$ ms)

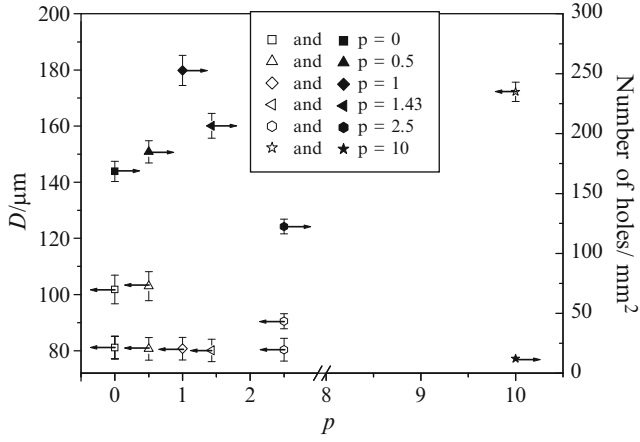

Fig. 4.22 The average diameter, D, and the number of holes per mm^2 surface area of copper electrodes obtained at a constant current density of 0.44 A/cm^2 and for different pause to pulse ratios. Pause duration: 10 ms (Reprinted from [30] with permission from Elsevier.)

corresponds to suppressed coalescence of hydrogen bubbles. The decrease of the number of holes and the appearing of dish-like holes can be ascribed to the decrease of quantity of evolved hydrogen and hence to the decrease of the effectiveness of solution stirring by evolved hydrogen with the increasing pause to pulse ratio.

Cauliflower-like agglomerates of copper grains can be classified into two groups. In the first group are inserted cauliflower-like agglomerates of copper grains constructing the honeycomb-like structures. These copper agglomerates are very disperse and consisted of small agglomerates of copper grains, as shown in Fig. 4.23a which shows the typical cauliflower-like agglomerates of copper grains obtained by the square-wave PC with a deposition pulse of 10 ms. From Fig. 4.23a can be seen that the size of these small copper grains agglomerates of which large cauliflower-like agglomerates formed among holes were constructed was about 4 μm. Also, the agglomerates of copper grains were surrounded by irregular channels for which the origin was of evolved hydrogen. In the second group are inserted cauliflower-like agglomerates

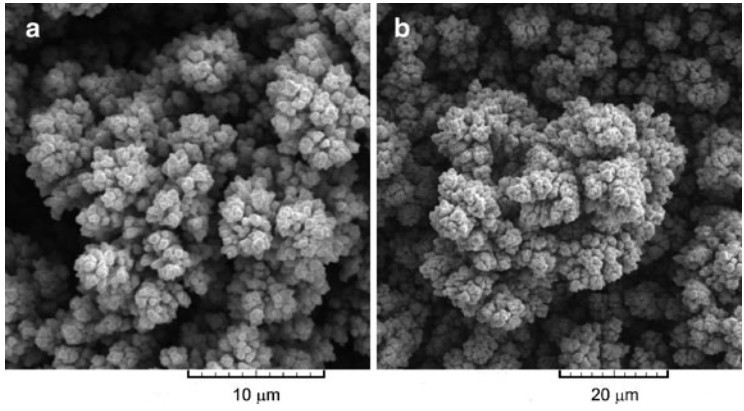

Fig. 4.23 The typical cauliflower-like agglomerates of copper grains formed by the PC regimes with a deposition pulse of: (**a**) 10 ms and (**b**) 1 ms. Pause duration: 10 ms (Reprinted from [30] with permission from Elsevier.)

of copper grains formed by the PC regime with a deposition pulse of 1 ms. Also, this type of agglomerates can be noticed in the transitional structure formed with a deposition pulse of 4 ms. The typical agglomerate of copper grains from this group is given in Fig. 4.23b which shows the one obtained with a deposition pulse of 1 ms. Copper grains agglomerates from this group are formed at the electrode surface independently from the formed hydrogen bubbles. They were larger and more compact than those formed among hydrogen bubbles at the constant current density and by the PC regimes with deposition pulses of 7, 10, and 20 ms [30].

Cross section of copper deposits obtained with deposition pulses of 4, 7, 10, and 20 ms is shown in Fig. 4.24. From Fig. 4.24, it can be seen that the interior of these structures was very porous and consisted of disperse particles surrounded by irregular channels for which the origin is of evolved hydrogen [44]. Also, it is necessary to note that dendritic character of these particles decreased with the prolonging duration of deposition pulse. As already mentioned, the porous interior of these deposits is very important for electrocatalytic purposes because the pores facilitate the transport of electroactive species through the interior of the structures, what is very desirable

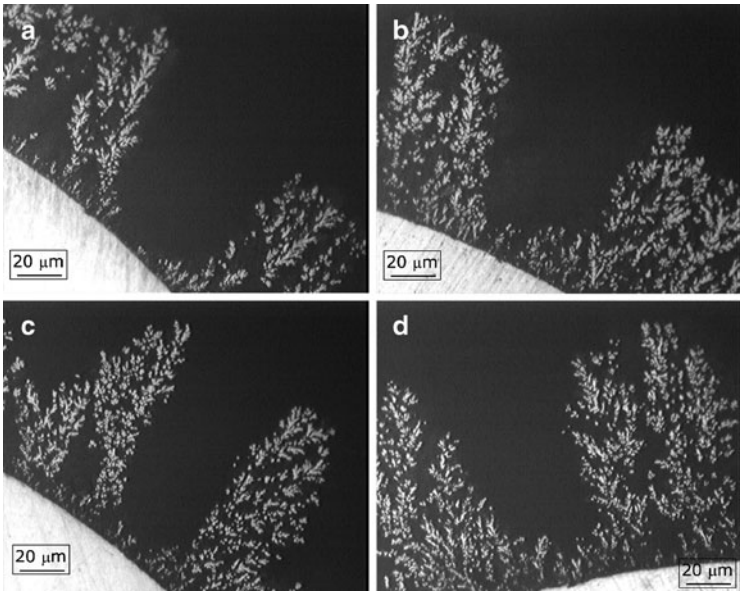

Fig. 4.24 Cross section of the copper deposits obtained by the PC regimes with deposition pulses of: (**a**) 4 ms; (**b**) 7 ms; (**c**) 10 ms; and (**d**) 20 ms. The current density amplitude: 0.44 A/cm^2. Pause duration: 10 ms (Reprinted from [44] with permission from Springer.)

for the evaluation of electrochemical reactions. For example, copper shows a high activity for nitrate ion reduction [46, 47], as well as for a reaction in which nitrate reduces to ammonia in high yield in aqueous acidic perchlorate and sulfate media [48].

4.6.1.3 Discussion of the Effect of Different Parameters of the PC Regimes on Electrodeposition of Copper in the Hydrogen Codeposition Range

From the above consideration, the existence of the strong effect of the selected parameters of the square-waves PC on hydrogen evolution reaction and hence morphology of electrodeposited copper is very

clear. The change of morphology of electrodeposited copper from very branchy dendrites and dish-like holes to the honeycomb-like structures can be explained by the analysis of the effectiveness of solution stirring by evolved hydrogen in the following way: the effectiveness of stirring of the solution by hydrogen generated at the cathode surface during electrochemical deposition process increases with intensification of hydrogen evolution reaction. In the one moment, hydrogen evolution will become vigorous enough to cause the decrease of the cathode diffusion layer thickness and the increase of the limiting diffusion current density leading to the change of the hydrodynamic conditions in the near-electrode layer [16]. According to Eqs. (4.5) and (4.10), it means the decrease of the degree of diffusion control of electrodeposition process with intensification of hydrogen evolution reaction. The degree of diffusion control of electrodeposition process will additionally decrease due to the smaller values of the effective average current densities, j_{av}*, in relation to those obtained in the absence of hydrogen evolution [Eqs. (4.3) and (4.13)]. Then, the overpotential amplitude corresponding to copper electrodeposition will be smaller than the one specified by pulse rectifiers and this value is denoted as effective overpotential amplitude of electrodeposition process and it is presented by Eq. (4.15).

Hence, the effective overpotential amplitude, $\eta_{A,eff}$, decreases with the intensification of hydrogen evolution reaction due to the decrease of the degree of diffusion control of electrodeposition process. So, the validity of the concept of "effective overpotential" can be expanded to include metal electrodeposition in the hydrogen codeposition range by the regime of pulsating current (PC), and then this concept applied for the PC regimes can be denoted as "effective overpotential amplitude" one [44].

Anyway, the decrease of dendritic character of particles and hence the increase of dispersity of particles in the formed honeycomb-like structures (Fig. 4.24), as well as the change of the surface morphology from dendrites (Fig. 4.19a) to agglomerates of grains formed around holes (Fig. 4.23a), clearly confirm the decrease of the degree of the diffusion control of electrodeposition process with the increase of the quantity of evolved hydrogen. The different degree of diffusion

control of electrodeposition process is attained by the choice of parameters of the square-waves PC. For example, using the value $j_A = 0.20$ A/cm^2, $t_c = 1$ ms, and $t_p = 10$ ms, as well as $\eta_{I,av}(H_2) = 5.5\%$, the effective average current density, j_{av}*, calculated by the use of Eq. (4.13) was very close to the value of the limiting diffusion current density for this system (i.e., for 0.15 M $CuSO_4$ in 0.50 M H_2SO_4; $j_L \approx 16.0$ mA/cm^2) [16]. Hence, with these parameters of the PC regimes, electrodeposition process was controlled by the diffusion of ions to the electrode surface, what is confirmed by the formation of very branchy dendrites and small cauliflower-like agglomerates of copper grains (Fig. 4.19a). Anyway, the nonuniformity of the electrode surface clearly pointed out that the diffusion layer of the macroelectrode was not disturbed by evolved hydrogen during this electrodeposition process.

On the other hand, the increase of the effectiveness of solution stirring, the decrease of the cathode diffusion layer thickness, and the increase of the limiting diffusion current density occur with the intensification of hydrogen evolution reaction leading to the formation of the honeycomb-like structures. The uniform distribution of morphological forms, i.e., holes and copper grains agglomerates, means the existence of the same hydrodynamic conditions over the whole electrode surface [19]. The size of grains in cauliflower-like agglomerates approached to nanosized dimensions with the intensification of hydrogen evolution reaction, as shown in Fig. 4.25 for cauliflower-like ones obtained with $t_c = 20$ ms. From Fig. 4.25, it can be clearly seen that the size of grains in these agglomerates is between 100 and 300 nm. Also, the porosity of the honeycomb-like structures was additionally increased by numerous nanopores situated between copper grains, as observed from Fig. 4.25. The increased effectiveness of the solution stirring by evolved hydrogen with the intensification of hydrogen evolution can also be noticed by the analysis of the internal structures of the honeycomb-like deposits shown in Fig. 4.24. The decrease of dendritic character of particles and hence the increase of dispersity of deposits is just a consequence of the increased effectiveness of the solution stirring by evolved hydrogen with the intensification of hydrogen evolution reaction caused by the prolongation of deposition pulse duration.

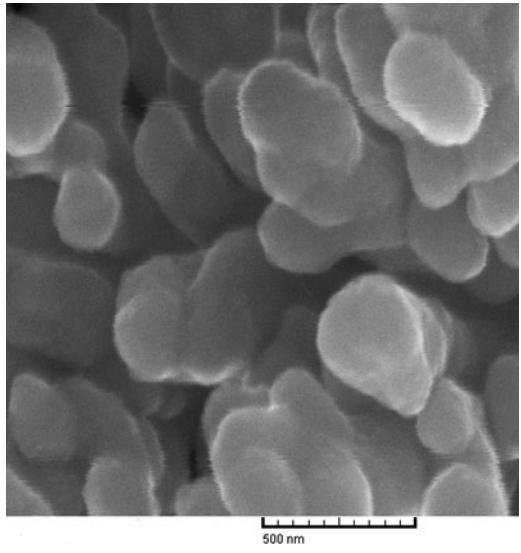

Fig. 4.25 Copper grains agglomerates obtained by the PC regime with a current density amplitude of 0.44 A/cm^2, a deposition pulse of 20 ms, and a pause duration of 10 ms (Reprinted from [44] with permission from Springer.)

4.6.2 Optimization of the Formation of the Honeycomb-Like Structure by the PC Regime

For the galvanostatic mode of operation, the specific energy consumption, w, defined as the energy spent in the process per unit mass of deposited copper, may be expressed according to [49] by Eq. (4.16):

$$w = \frac{nF\int_0^t U(t)\mathrm{d}t}{M\int_0^t \eta_{\mathrm{I,Cu}}(t)\mathrm{d}t} \tag{4.16}$$

or by Eq. (4.17) as

$$w = \frac{nFU_{\mathrm{av}}}{M\eta_{\mathrm{I,av}}(\mathrm{Cu})}, \tag{4.17}$$

where

$$U_{\mathrm{av}} = (1/t)\int_0^t U(t)\mathrm{d}t \tag{4.18}$$

and

$$\eta_{\mathrm{I,av}}(\mathrm{Cu}) = (1/t)\int_0^t \eta_{\mathrm{I,Cu}}(t)\mathrm{d}t. \tag{4.19}$$

According to Eq. (4.17) the specific energy consumption depends on the average cell voltage, U_{av}, and the average current efficiency for copper electrodeposition reaction, $\eta_{\mathrm{I,av}}(\mathrm{Cu})$. The values of the average current efficiencies for copper electrodeposition, $\eta_{\mathrm{I,av}}(\mathrm{Cu})$, were calculated using data from Table 4.2 as $\eta_{\mathrm{I,av}}(\mathrm{Cu}) = 100–\eta_{\mathrm{I,av}}(\mathrm{H_2})$, and the obtained values are added to Table 4.2. The values of the average cell voltages, U_{av}, can be calculated by Eq. (4.18) using the experimentally determined dependences of the cell voltages, U, on time t [30]. The tendency of the decrease of the average cell voltages was observed with the shortening deposition pulse and these values were smaller than the average cell voltage obtained at constant current density of 0.44 A/cm^2 [30].

In square-wave PC regimes, the average current density and the average cell voltage depend on pause to pulse ratio in a similar way. Hence, the average cell voltage, U_{av}, in a function of p can be given by Eq. (4.20) [34, 35]:

$$U_{\mathrm{av}} = \frac{U_{\mathrm{A}}}{p+1}, \tag{4.20}$$

where U_{A} is the amplitude cell voltage, if there is no rest cell voltage during pause duration. In this study, the constant current density used in DC regime ($j = 0.44$ A/cm^2) was equal to the amplitude of current density in the PC regimes. Consequently, the cell voltage in the DC regime was used as the amplitude value in the PC regimes [30]. Then, the amplitude cell voltage, U_{A}, can be calculated as $U_{\mathrm{A}} = (1/t)\int_0^t U(t)\mathrm{d}t$, where U is the cell voltage in a time t for a constant regime of electrolysis, and the value of 1.1 V was obtained.

Anyway, the difference between the experimentally determined dependences and calculated in this way was observed and it can be ascribed to the existence of rest voltage during pause. Due to this rest voltage making the cell voltage during pause to be higher than zero, the amplitude cell voltage cannot be calculated by the experimentally measured average cell voltage using Eq. (4.20).

For that reason, assuming that the value of the peak voltage during deposition pulse will not be higher than the cell voltage in constant current mode, the average cell voltage obtained at the constant current density ($p = 0$) was used for the calculation of the specific energy consumption. Then, using the values of the average current efficiencies for copper electrodeposition reaction from Table 4.2 and the average cell voltage of 1.1 V obtained at the constant current density of 0.44 A/cm^2, the values of the specific energy consumption are calculated and added to Table 4.2.

From Table 4.2, it can be seen that the shortening of deposition pulse led to the decrease of the specific energy consumption, and the obtained values were smaller than the one obtained in the constant mode. On the other hand, the increasing deposition pulse duration favored the formation of the honeycomb-like electrodes. This enabled the optimization process of the formation of the honeycomb-like copper electrodes by the choice of the appropriate parameters of square-waves PC. As already mentioned, the honeycomb-like structures were formed with the pause to pulse ratio smaller than 1.43 (or with the deposition pulse of 7 ms and larger, and a pause duration of 10 ms). It is clear that energy saving of 15.3% was attained by the production of the honeycomb-like electrode by the square-wave PC with a deposition pulse of 7 ms ($p = 1.43$) in comparison to the one obtained at the constant current density. Simultaneously, the increase of the specific surface area of the honeycomb-like electrodes, manifested by the increase of the number of holes due to the suppressed coalescence of closely formed hydrogen bubbles, was observed by the application of these PC regimes (Fig. 4.22).

Anyway, the use of the appropriate square-waves PC enabled energy saving in the production of the honeycomb-like electrodes. In this moment, the largest problem for the commercial manufacturing of open porous structures by the PC regimes is high cost of a pulse rectifier which is much greater than a DC unit [50].

It is a highly regulated and sophisticated design that costs more to manufacture. At the first sight, energy savings attained by the application of the PC regimes and high cost of production of pulse rectifier are in contradiction, but further development of the electronic industry will probably decrease the cost of these rectifiers and will enable their larger application in electrochemical technologies.

For the technological application of open porous structures as possible electrodes in electrochemical devices, the deposit structural stability of these deposits determined by their adhesion with electrode surface is also very important. It is a well-known fact that the adhesion of deposits is closely associated with the quantity of hydrogen by which metal deposits are formed [51]. At high current densities, dendritic deposits are initiated on the cathode with simultaneous evolution of hydrogen gas. At higher current density, the deposit structure becomes more open, nonuniform, and finer, due to the increased nucleation rate and hydrogen evolution on the cathode [51]. Also, similar effects on copper deposit morphology are observed in potentiostatic regime of electrolysis. Increasing overpotential intensifies the hydrogen evolution reaction causing the change of morphology of electrodeposited copper from dendrite to the honeycomb-like structure constructed of holes formed by the attached hydrogen bubbles with cauliflower-like copper grains agglomerates among them [16]. The mechanical strength of the copper deposits decreases with the increasing current density and hence with the increasing quantity of evolved hydrogen what is proven by the measurement of adhesion of copper deposits by the peel strength test [51]. Hence, it can be concluded by this analysis that the mechanical strength of the honeycomb-like copper structures was improved by the application of PC regimes due to the decrease of the average current efficiency of hydrogen evolution by which they are formed.

Hence, the following conveniences in the production of open porous structures, denoted as 3-D foam or the honeycomb-like one, are attained since the appropriate square-waves PC parameters were selected: (a) energy saving, (b) the increase of the specific surface area of the electrodes, and (c) probably the improvement of the deposit structural stability due to the decrease of the quantity of evolved hydrogen needed for their formation. Also, it is clear that the

benefits attained by the application of the pulsating overpotential (PO) regime can be succesfully transferred to technological attractive pulsating current (PC) regime.

4.7 The Regime of Reversing Current

The regime of reversing current (RC) is characterized by the cathodic current density, j_c, and the anodic current density, j_a, as well as by the duration of flow of the current in the cathodic and the anodic directions, t_c and t_a, respectively [34, 35]. The average current density, j_{av}, is given by Eq. (4.21):

$$j_{av} = \frac{j_c t_c - j_a t_a}{t_c + t_a} \tag{4.21}$$

or

$$j_{av} = \frac{j_c - j_a r}{1 + r}, \tag{4.22}$$

if

$$r = \frac{t_a}{t_c}. \tag{4.23}$$

For the RC regime in the millisecond range, the surface concentration of the depositing ions is determined by the average current density [34, 35], and the overpotential amplitude, η_A, can be presented by Eq. (4.24):

$$\eta_A = \frac{b_c}{2.3} \ln \frac{j_{av}(r+1) + j_a r}{j_0} + \frac{b_c}{2.3} \ln \frac{1}{1 - \frac{j_{av}}{j_L}}. \tag{4.24}$$

Equation (4.24) is valid in the frequency range 10–100 Hz, where the frequency is sufficiently high to produce constant concentration

on the surface and sufficiently low that the effect of DC capacity can be neglected. It is noteworthy that it is valid if $j_{av} < j_L$ in the mixed controlled deposition.

With the applied cathodic current density pulses larger than the limiting diffusion current density, parallel to copper electrodeposition hydrogen evolution reaction occurs [52]. On the other hand, there was not any gas evolution during anodic pulses indicating that the overall gas evolution corresponds to hydrogen evolution. Then, Eq. (4.22) can be modified by Eq. (4.25):

$$j_{av}* = \frac{\eta_{I,c}(Cu) j_c - j_a r}{1 + r}, \tag{4.25}$$

where j_{av}* is the effective average current density and $\eta_{I,c}(Cu)$ is the current efficiency for copper electrodeposition during cathodic pulses. Since $\eta_{I,c}(Cu) + \eta_{I,c}(H_2) = 1$, Eq. (4.25) can be presented as

$$j_{av}* = \frac{[1 - \eta_{I,c}(H_2)] j_c - j_a r}{1 + r}, \tag{4.26}$$

where $\eta_{I,c}(H_2)$ is the current efficiency for hydrogen evolution reaction during cathodic pulses. For $j_{av}* > j_L$, the overpotential amplitude is related to the hydrogen reduction, increasing with the current density of hydrogen evolution [43], and the modified Eq. (4.24) can be presented as

$$\eta_{A,eff} = \frac{b_c}{2.3} \ln \frac{j_{av} * (r + 1) + j_a r}{j_0} + \frac{b_c}{2.3} \ln \frac{1}{1 - \frac{j_{av}*}{j_L*}}, \tag{4.27}$$

where $\eta_{A,eff}$ is the effective overpotential amplitude and j_L* is the effective limiting diffusion current density. Naturally, $j_{av}* < j_L*$.

The regime of pulsating current (PC) represents the special case of the reversing current (RC) regime ($j_a = 0$ mA/cm^2). For that reason, copper electrodeposition processes in the hydrogen codeposition range by the RC regimes with the different anodic current density values are compared with those obtained by the PC regime.

Table 4.3 The values of the average current efficiencies of hydrogen evolution, $\eta_{I,av}(H_2)$, in %, obtained for electrodeposition of copper with different anodic current densities

j_a (mA/cm^2)	0	40	240	440	640
$\eta_{I,av}(H_2)$ (%)	30.7	28.9	25.6	21.7	19.3

Reprinted from [52] with permission from Elsevier
j_a the anodic current density in mA/cm^2

4.7.1 The Effect of the Anodic Current Density on the Formation of the Honeycomb-Like Electrodes

In all PC and RC experiments, the cathodic current density (or the current density amplitude in the PC regime) of 0.44 A/cm^2, the cathodic time (or deposition pulse) of 10 ms, and the anodic time (or pause duration) of 5 ms were applied, while the analyzed anodic current densities were 0.040, 0.24, 0.44, and 0.64 A/cm^2. Copper was electrodeposited from 0.15 M $CuSO_4$ in 0.50 M H_2SO_4 at the room temperature using cylindrical copper working electrodes. The values of the average current efficiencies of hydrogen evolution calculated as $\eta_{I,av}(H_2) = (1/t)\int_0^t \eta_I(H_2)dt$ for the analyzed PC and RC regimes are presented in Table 4.3.

Morphologies of copper deposits obtained by the PC regime and RC regimes with different anodic current densities are shown in Fig. 4.26. Holes formed of detached hydrogen bubbles and agglomerates of copper grains or dendrites were obtained with all analyzed PC and RC regimes. From Fig. 4.26, it can be seen that the honeycomb-like structures are formed by the PC regime and by the RC regimes with the anodic current densities up to 440 mA/cm^2. Holes obtained by a coalescence of closely formed hydrogen bubbles are noticed by the analysis of the honeycomb-like structures formed by the PC regime (Fig. 4.27a) and the RC regime with j_a of 40 mA/cm^2. In the range of the examined anodic current densities from 0 (the PC regime) to 440 mA/cm^2, holes constructing the honeycomb-like structures (so-called "noncoalesced" one) were similar to each other, and the typical hole of this type obtained with

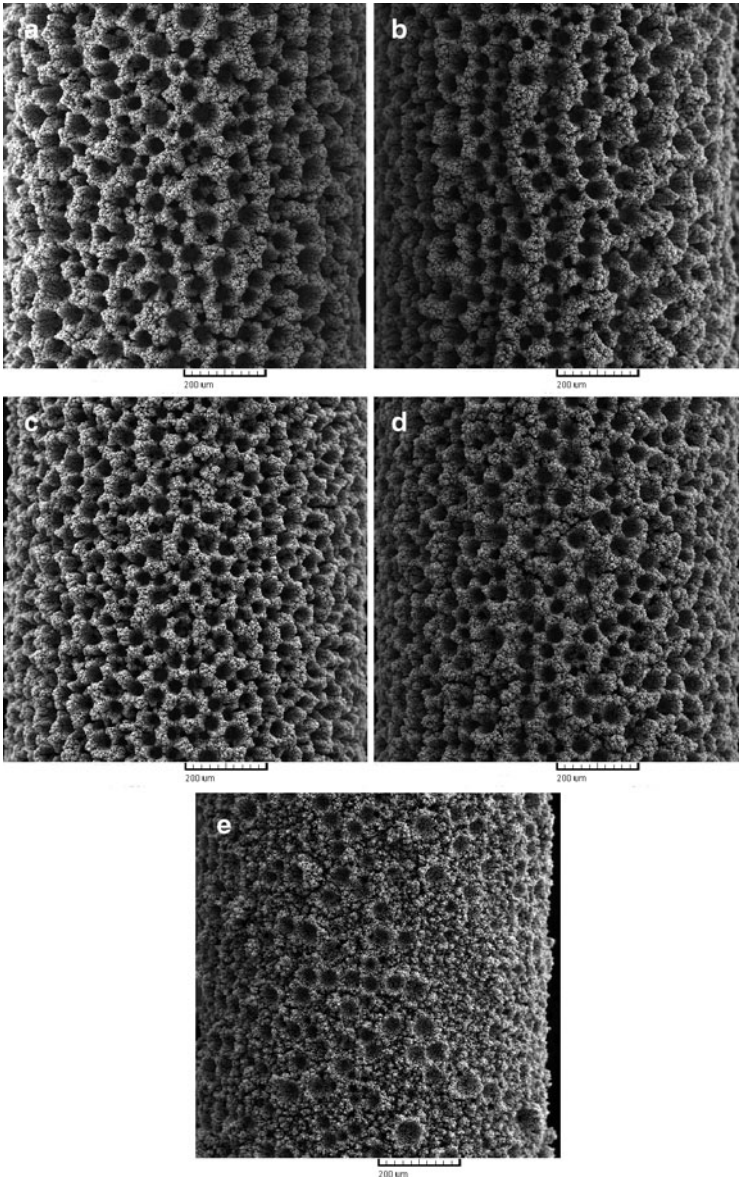

Fig. 4.26 Copper deposits obtained by: (**a**) the PC regime and by the RC regimes with the anodic current density j_a of: (**b**) 40; (**c**) 240; (**d**) 440 and (**e**) 640 mA/cm^2. The cathodic current density j_c: 440 mA/cm^2, the cathodic pulse t_c: 10 ms, and the anodic pulse, t_a: 5 ms (Reprinted from [52] with permission from Elsevier.)

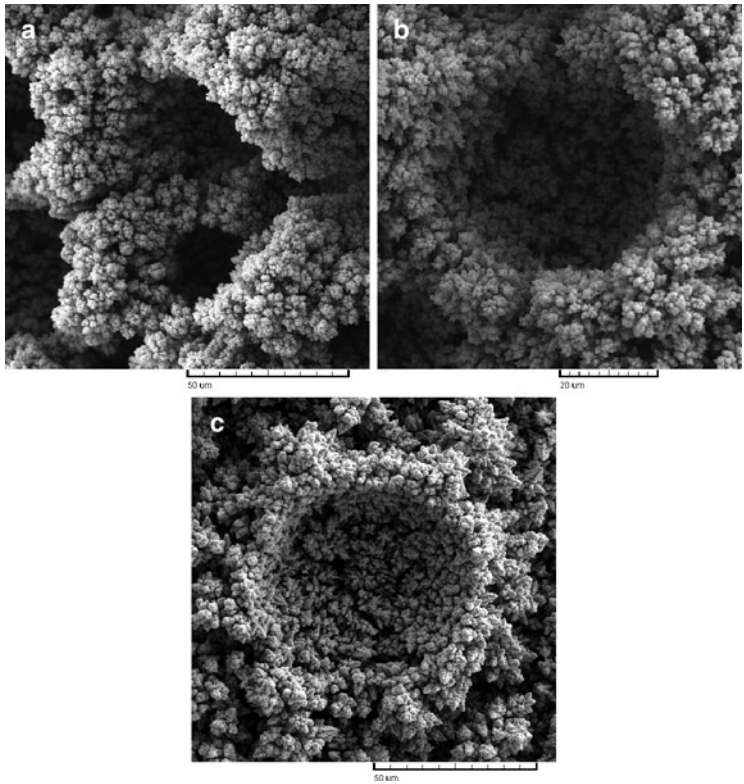

Fig. 4.27 The types of holes formed of detached hydrogen bubbles by different PC and RC regimes: (**a**) coalesced hole obtained by the PC regime; (**b**) noncoalesced hole obtained by the RC regime with $j_a = 440$ mA/cm^2 and (**c**) dish-like hole obtained by the RC regime with $j_a = 640$ mA/cm^2. The cathodic current density j_c: 440 mA/cm^2, the cathodic pulse t_c: 10 ms, and the anodic pulse, t_a: 5 ms (Reprinted from [52] with permission from Elsevier.)

j_a of 440 mA/cm^2 is shown in Fig. 4.27b. Finally, dish-like holes were dominant type of holes obtained with j_a of 640 mA/cm^2 (Fig. 4.27c).

Figure 4.28 shows the dependences of the average diameter and the number of holes formed at electrode surface in a function of the anodic current density. The average size and number of holes obtained for the PC regime ($j_a = 0$ mA/cm^2) are also included in this figure.

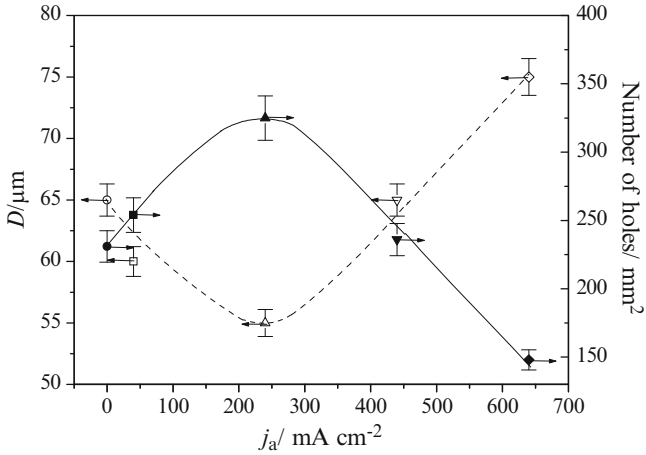

Fig. 4.28 The dependences of the average diameter, D, and the number of holes per mm^2 surface area of copper electrodes on the anodic current density value. The cathodic current density j_c: 440 mA/cm^2, the cathodic pulse t_c: 10 ms, and the anodic pulse t_a: 5 ms (Reprinted from [52] with permission from Elsevier.)

The average diameter of holes obtained by coalescence of closely formed hydrogen bubbles was larger than the average diameter of "noncoalesced" holes, and the size of these holes is not presented in Fig. 4.28. From Fig. 4.28, it can be seen that the dependence of the average diameter of holes on the anodic current density is of a parabolic shape with a minimum at $j_a = 240$ mA/cm^2. On the other hand, the dependence of the number of the holes per mm^2 surface area of the electrode on the anodic current density value had the shape of reverse parabola with the maximal number of holes formed with $j_a = 240$ mA/cm^2. Due to the existence of holes formed by coalescence process, the overall number of holes formed by both the PC regime and the RC regime with $j_a = 40$ mA/cm^2 was smaller than the one formed by the RC regime with $j_a = 240$ mA/cm^2. The decrease of the number of holes with the anodic current density larger than $j_a = 240$ mA/cm^2 can be ascribed to the strong effect of the anodic current densities on both the hydrogen evolution reaction and copper electrodeposition rate.

Morphologies of copper deposits formed around holes are shown in Fig. 4.29. The change of morphology of the electrodeposited copper from cauliflower-like agglomerates of copper grains to dendrites was observed with the increasing anodic current density values. Cauliflower-like agglomerates of copper grains obtained by the regimes of PC (Fig. 4.29a) and RC with $j_a = 40$ mA/cm^2 (Fig. 4.29b) are very disperse, and the presence of deep irregular channels of detached hydrogen bubbles [19] formed around small copper grains agglomerates was easily noticed. From Fig. 4.29a, b, it can be clearly seen that these cauliflower-like agglomerates of copper grains are very similar to each other, what is understandable due to the absence or the small value of the anodic component of the current density in comparison with the cathodic current density. With the increasing anodic current density, deep irregular channels around small copper agglomerates were lost making the honeycomb-like structures obtained with $j_a = 240$ mA/cm^2 (Fig. 4.26c) and $j_a = 440$ mA/cm^2 (Fig. 4.26d) more compact than those obtained in the PC regime (Fig. 4.26a) and the RC regime with $j_a = 40$ mA/cm^2 (Fig. 4.26b). Also, holes approached each other (or the wall width decreased) with the increase of the anodic current density (Fig. 4.29a–c). The increase of the anodic current density led to the formation of dendrites on the top of agglomerates of copper grains (Fig. 4.29d). Finally, very branchy dendrites were formed with $j_a = 640$ mA/cm^2 (Fig. 4.29e).

The increase of the compactness of the honeycomb-like structures can be explained by the strong effect of the anodic current density on both the hydrogen evolution reaction and copper electrodeposition rate as follows: in the growth process, due to the current density distribution effect, during cathodic pulses both the copper nuclei and the hydrogen bubbles are primarily formed at the top of agglomerates of grains formed around initially formed hydrogen bubbles. During anodic pulses, due to the same effect, the anodic current density (or the anodic current lines) will be concentrated at the top of these freshly formed copper nuclei causing their dissolution. The dissolution process of copper nuclei facilitates to freshly formed hydrogen bubbles to find path to coalesce with initially formed hydrogen bubbles leading to their growth with electrolysis time. With the increasing anodic current density, the dissolution of copper

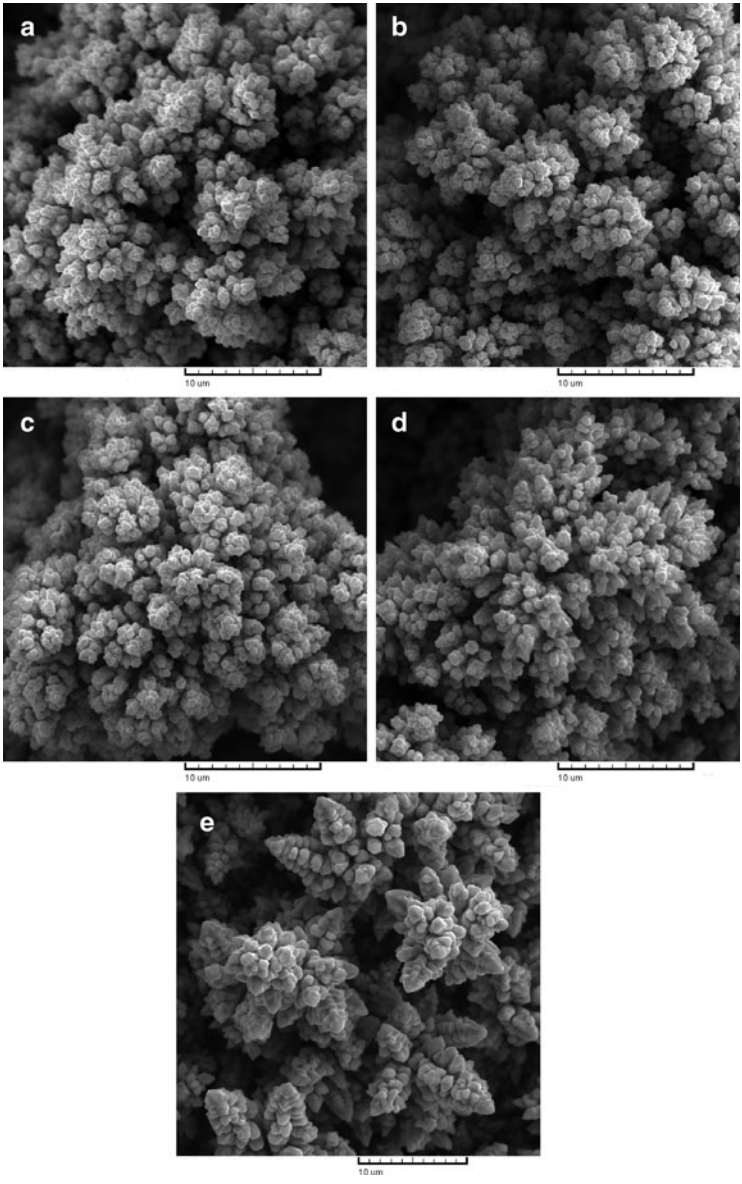

Fig. 4.29 Morphology of electrodeposited copper formed around holes by: (**a**) the PC regime and by the RC regimes with the anodic current density j_a of: (**b**) 40; (**c**) 240; (**d**) 440 and (**e**) 640 mA/cm^2. The cathodic current density j_c: 440 mA/cm^2, the cathodic pulse t_c: 10 ms, and the anodic pulse t_a: 5 ms (Reprinted from [52] with permission from Elsevier.)

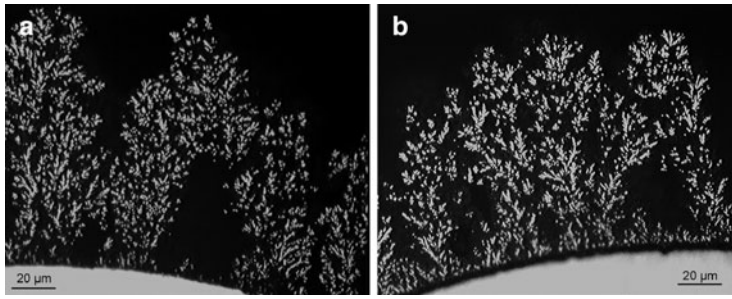

Fig. 4.30 Cross section of the honeycomb-like deposits obtained with: (**a**) j_a = 40 mA/cm^2 and (**b**) j_a = 440 mA/cm^2. The cathodic current density j_c: 440 mA/cm^2, the cathodic pulse t_c: 10 ms, and the anodic pulse t_a: 5 ms (Reprinted from [52] with permission from Elsevier.)

nuclei increases, and the number of freshly formed hydrogen bubbles which will coalesce with the initially formed hydrogen bubbles is increased. Simultaneously, the number of hydrogen bubbles which will remain trapped among freshly formed copper nuclei and constructing channel structure through the interior of the deposit is decreased. It means that these simultaneous processes will lead to a reduction of irregular channels formed around small copper grains agglomerates, and hence, up to the increase of the compactness of the honeycomb-like structures.

Anyway, the ratio of hydrogen creating channel structure to the overall quantity of evolved hydrogen decreases with the increasing anodic current density values. Also, due to the increasing dissolution effect, the size of grains constructing agglomerates decreased with the increase of the anodic current density.

The complete insight into the strong effect of the anodic current density on the macromorphology of copper deposits is obtained by the analysis of their internal structures. Figure 4.30 shows cross sections of the honeycomb-like deposits obtained with j_a = 40 mA/cm^2 (Fig. 4.30a) and j_a = 440 mA/cm^2 (Fig. 4.30b). At the first sight, a clear difference in the internal structures of these copper deposits can be seen by the analysis of Fig. 4.30. The interior of copper deposit obtained with j_a = 40 mA/cm^2 was constructed from fine particles (Fig. 4.30a), while a well-defined dendritic structure can be noticed in

the copper deposit obtained with $j_a = 440$ mA/cm^2 (Fig. 4.30b). The second strong effect of the increasing anodic current density on the internal structure of the copper deposits was related to the shape of cavities formed in the interior of deposits. The absence of the deposit at the bottom of the cavity and its regular shape close to the electrode surface following the shape of hydrogen bubbles clearly indicate that the origin of the cavity in the deposit obtained with $j_a = 40$ mA/cm^2 is of hydrogen bubbles formed at the electrode surface in the initial stage of electrodeposition. The formed hydrogen bubbles isolate the electrode surface preventing the growth of deposit at the position of their formation. In the growth process, due to the current density distribution effect, they remained included in the interior of deposit making this deposit type to be very porous. This type of cavity is not found in the copper deposits obtained with the larger anodic current densities indicating that the increase of the number of holes formed of detached hydrogen bubbles (Fig. 4.28) can be not only ascribed to suppressed coalescence of closely formed hydrogen bubbles but also to the improved current density distribution at the growing electrode surface. The second type of the cavity had irregular shape (Fig. 4.30b) and this cavity type is formed by the overlap of closely formed branchy dendrites. From Fig. 4.30b, it can be seen that before the overlap of dendrites, copper electrodeposition occured over the whole electrode surface. The improvement of the current density distribution effect was observed with the increasing anodic current density.

The formation of dendrites instead of fine particles can be explained by the decrease of the quantity of the hydrogen generated during copper electrochemical deposition processes with the increase of the anodic current density as follows: due to the decrease of the quantity of evolved hydrogen which leads to a stirring of solution in the near-electrode layer, the thickness of the diffusion layer increases and the limiting diffusion current density decreases causing the increase of the degree of diffusion control of the electrodeposition process. From the point of view of mechanism of the electrodeposition processes in the hydrogen codeposition range, it means that the effective overpotential amplitude, $\eta_{A,eff}$ [Eq. (4.27)] will increase with the increasing anodic current density. The change of morphology of the electrodeposited copper from very disperse agglomerates of copper grains to branchy dendrites (Fig. 4.29) clearly points out

the increase of the degree of diffusion control of the electrodeposition process with the increasing anodic current density.

4.7.1.1 Analysis of the Applied Regimes of RC on Both the Specific Surface Area and the Structural Stability

On the basis of the maximal number of holes and the minimal wall width (or the distance among holes), it is clear that the largest specific surface area of the honeycomb-like electrode is obtained by the RC regime with $j_a = 240$ mA/cm^2.

As already mentioned, the average current efficiency of hydrogen evolution decreased with the increasing anodic current density. In the range of the anodic current densities from 0 (the PC regime) to 440 mA/cm^2 which enabled the formation of the honeycomb-like electrodes, the decrease of $\eta_{I,av}(H_2)$ of 29.3% was reached. The honeycomb-like electrode with the maximal specific surface area (the RC regime with $j_a = 240$ mA/cm^2) was formed with 16.6% smaller the average current efficiency of hydrogen evolution than the one obtained by the PC regime. The change of $\eta_{I,av}(H_2)$ was increased when the comparison between the average current efficiencies of hydrogen evolution obtained for the honeycomb-like structures formed in the constant galvanostatic regime at the current density which corresponded to the cathodic current density of 440 mA/cm^2 and the RC regime with $j_a = 240$ mA/cm^2 was made. In the constant regime of electrolysis, at $j = 440$ mA/cm^2, $\eta_{I,av}(H_2) = 36.0\%$ [30], and the decrease of $\eta_{I,av}(H_2)$ of 28.9% was obtained. It is well known fact that the structural stability of a deposit is closely associated with the quantity of hydrogen evolved at the electrode surface during the electrodeposition process [51]. The smaller the quantity of evolved hydrogen, the better structural stability of a deposit is obtained. The decrease of a quantity of evolved hydrogen spent for the formation of the honeycomb-like electrodes by the RC regime clearly indicates the improvement of the structural stability of these electrodes in relation to the one obtained by other regimes of electrolysis, such as the PC regime and the constant galvanostatic one.

Some of the advantages of the production of the honeycomb-like electrodes by the RC regime in relation to the constant galvanostatic and PC regimes are both the increase of the specific surface area and the improvement of their structural stability. It is clear that these advantages make this regime superior in relation to other regimes of electrolysis.

4.8 Comparison of Open Porous Copper Structures Obtained by Different Current Regimes of Electrolysis

Using the well-known fact that electrodeposition of metal by the PC and RC regimes in the millisecond range occurs at the average current density [34, 35], the formation of open porous copper structures by these regimes of electrolysis at the same average current density is examined. The obtained surface morphologies were compared with the one obtained in galvanostatic regime at the current density which was equal to the selected average current density. In all experiments for which results are presented here, copper electrodeposition was performed from 0.15 M $CuSO_4$ in 0.50 M H_2SO_4 at room temperature using cylindrical copper wires as working electrodes [53]. In all PC and RC experiments, the cathodic current density of 0.44 A/cm^2 and a deposition pulse of 10 ms were selected. The average current density, j_{av}, of 0.12 A/cm^2 was reached by a selection of pause duration of 26.6 ms [for the PC regime; see Eq. (4.3)], as well as by the regulation of ratios between the anodic current density j_a and the anodic pulse duration t_a [for the RC regimes; see Eq. (4.21)]. Then, the following j_a and t_a values were selected:

(a) $j_a = 0.040$ A/cm^2; $t_a = 20$ ms (denoted as RC40)
(b) $j_a = 0.20$ A/cm^2; $t_a = 10$ ms (denoted as RC200)
(c) $j_a = 0.52$ A/cm^2; $t_a = 5$ ms (denoted RC520)

Figure 4.31 shows the morphologies of electrodeposited copper obtained by the RC regimes (RC40—Fig. 4.31a; RC200—Fig. 4.31b;

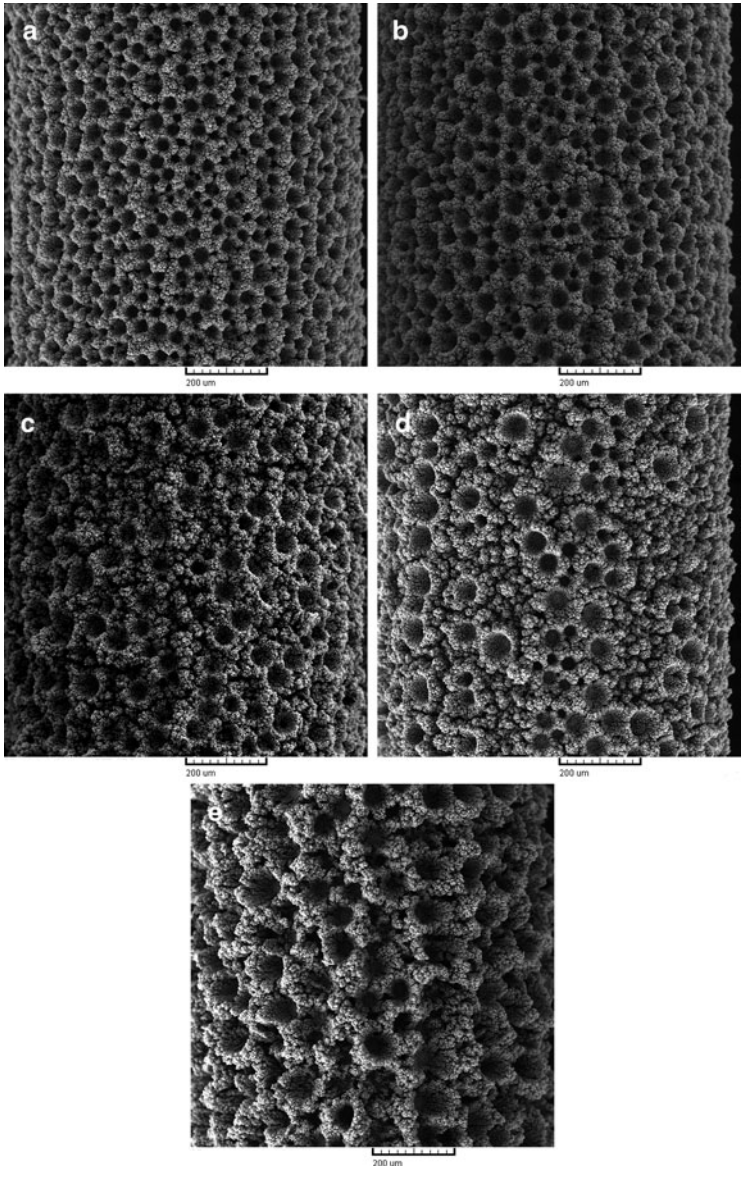

Fig. 4.31 Copper deposits obtained by: (**a**) RC40; (**b**) RC200; (**c**) RC520 regimes; (**d**) PC regime; and (**e**) the galvanostatic regime

and RC520—Fig. 4.31c), by the PC regime (PC—Fig. 4.31d); and in the constant galvanostatic regime (DC—Fig. 4.31e). As already mentioned, the average current density was the same in all analyzed PC and RC regimes, while the applied current density in the DC mode corresponded to the average current density in the PC and RC regimes. From Fig. 4.31, it can be seen that holes formed of detached hydrogen bubbles and cauliflower-like agglomerates of copper grains or dendrites were formed under these electrodeposition conditions. These copper deposits were formed by approximately the same quantity of evolved hydrogen which corresponded to $\eta_{I,av}(H_2)$ of $22.0 \pm 0.8\%$ [53]. It was understandable due to the fact that electrodeposition processes in the millisecond range at periodically changing rate occur at the average current density [34, 35].

The obtained surface morphologies can be classified into two groups. In the first group are the honeycomb-like structures obtained by the RC regimes, denoted as RC40 (Fig. 4.31a) and RC200 (Fig. 4.31b), as well as in the DC mode (Fig. 4.31e). The characteristic of the second group of the obtained copper deposits is the dominant presence of dish-like holes and independently formed cauliflower-like agglomerates of copper grains. These morphological forms were obtained by the RC520 (Fig. 4.31c) and PC (Fig. 4.31d) regimes.

From Fig. 4.31a, b, e, it can be seen a clear difference in the size and number of holes, as well as in the wall width among them in the honeycomb-like structures obtained by the RC40 and RC200 regimes and those obtained at a constant current density. The typical holes obtained by the RC40 and the DC mode are shown in Fig. 4.32a, b, respectively. The holes obtained by the RC40 and RC200 regimes were about twice smaller than those obtained at the constant current density. The average size of these holes was about 50 μm, while holes obtained in the DC mode were about 100 μm. Morphologies of deposits among holes obtained by the RC40 regime and the DC mode are shown in Fig. 4.32c, d, respectively. The cauliflower-like agglomerates of copper grains with small dendrites on them were formed by the RC40 (Fig. 4.32c) and RC200 regimes. The nucleation exclusion zones can be clearly observed around these cauliflower-like agglomerates of copper grains. On the other hand, the relatively large cauliflower-like copper grains agglomerates surrounded by

deep irregular channels for which the origin is of evolved hydrogen were formed in the DC mode (Fig. 4.32d). Anyway, it is clear that the application of appropriate RC regime led to the redistribution of evolved hydrogen favoring growth of hydrogen bubbles with electrolysis time and hence decreasing the contribution of generated hydrogen to the creating of channel structure through the interior of the deposit (the current density distribution effect).

Dish-like holes were the dominant type of holes obtained by the PC and RC520 regimes. The typical dish-like hole obtained by the PC regime is given in Fig. 4.32e. The average diameter of this type of holes was about 100 μm. The cauliflower-like agglomerates of copper grains, and the mixture of cauliflower-like copper grains agglomerates and dendrites were formed by the PC and RC520 regimes, respectively. The typical independently formed cauliflower-like agglomerate of copper grains obtained by the PC regime is presented in Fig. 4.32f.

From technological point of view, the first group of copper deposits (the honeycomb-like structures) is especially important for the application as electrodes in electrochemical devices [1] and in catalysis [3]. It is shown that the size of holes and wall width among holes were decreased, while the number of holes was increased when the appropriate RC parameters were applied (RC40 and RC200). In this way, the specific surface of the honeycomb-like electrodes was considerably increased confirming superiority the regime of reversing current in relation to other current regimes of electrolysis (the PC regime and the constant galvanostatic regime).

Comparing all periodically changing regimes of electrolysis, it can be noticed that the effects attained by the application of the RC regimes on microstructural characteristics of the honeycomb-like structures were more similar to those attained by the regime of pulsating overpotential (PO) than those attained by the pulsating current (PC) regime. It was understandable due to the existence of anodic current during "off period" in the PO regimes [37].

Anyway, from the point of view of the formation of the honeycomb-like electrodes by the electrodeposition techniques, the regime of reversing current is more suitable than other current regimes of electrolysis.

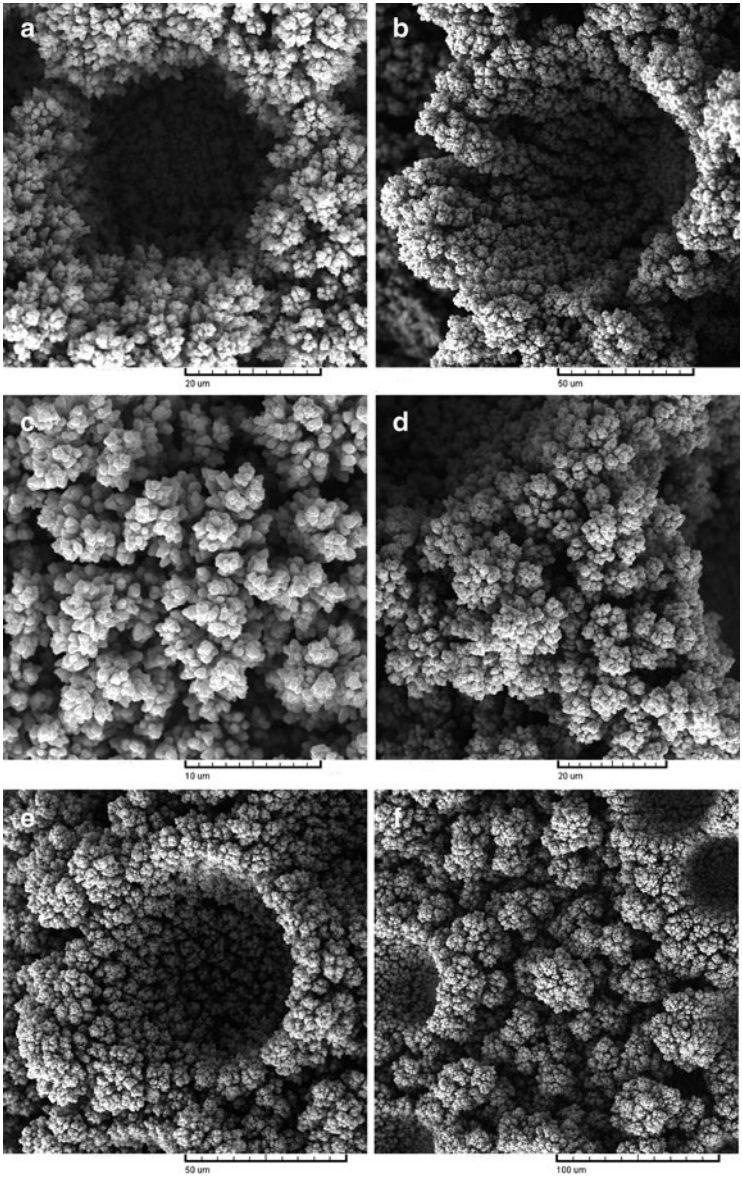

Fig. 4.32 The typical holes obtained by (**a**) RC40, (**b**) galvanostatic, and (**e**) PC regimes and morphological forms obtained among holes by (**c**) RC40, (**d**) galvanostatic, and (**f**) PC regimes

4.9 Conclusions

The comprehensive survey of the formation of open porous copper structures by both the constant and periodically changing regimes of electrolysis is presented. The main characteristics of this structure type, denoted as the honeycomb-like or the 3D foam ones, are holes or pores formed of detached hydrogen bubbles surrounded by cauliflower-like agglomerates of copper grains or dendrites. In the constant regimes of electrolysis, these structures are formed at overpotentials outside the plateau of the limiting diffusion current density (the potentiostatic regime) or current densities higher than the limiting diffusion current density (the galvanostatic regime), where parallel to copper electrodeposition hydrogen evolution reaction occurs. The number, size, and distribution of holes in the honeycomb-like structures depended on the Cu(II) ions and H_2SO_4 concentrations, temperature of electrolysis, the type of the working electrode used, and a time of electrolysis.

In periodically changing regimes of electrolysis, such as the pulsating overpotential (PO), the pulsating current (PC), and the reversing current (RC) regimes, the overpotential amplitude (in the PO regime), the current density amplitude (in the PC regime), or the cathodic current density (in the RC regime) is outside (the PO regime) or higher than the limiting diffusion current density (the PC and RC regimes). The following conveniences in the production of the honeycomb-like structures can be attained since the appropriate square-waves parameters of periodically changing regimes of electrolysis are selected (a) energy saving; (b) the increase of the specific surface area of the electrodes; and (c) probably the improvement of the deposit structural stability due to the decrease of the quantity of evolved hydrogen needed for their formation.

Acknowledgments The author is grateful to Prof. Dr. Konstantin I. Popov for helpful discussion during the preparation of this chapter.

Also, the author is grateful to Dr. Goran Branković and Dr. Ljubica Pavlović for SEM analysis of investigated systems, as well as to Dr. Vesna Maksimović for the cross section analysis of the obtained deposits.

The work was supported by the Ministry of Education and Science of the Republic of Serbia under the research project "Electrochemical synthesis and characterization of nanostructured functional materials for application in new technologies" (No. 172046).

References

1. Shin H-C, Dong J, Liu M (2003) Adv Mater 15:1610
2. Shin H-C, Liu M (2005) Adv Funct Mater 15:582
3. Yin J, Jia J, Zhu L (2008) Int J Hydrogen Energy 33:7444
4. Shin H-C, Liu M (2004) Chem Mater 16:5460
5. Li Y, Jia W-Z, Song Y-Y, Xia XH (2007) Chem Mater 19:5758
6. Guo YL, Yui H, Minamikawa H, Yang B, Masuda M, Ito K, Shimizu T (2006) Chem Mater 18:1577
7. Kazeminezhad I, Barnes AC, Holbrey JD, Seddon KR, Schwarzacher W (2007) Appl Phys A Mater Sci Process 86:373
8. Yuan JH, He FY, Sun DC, Xia XH (2004) Chem Mater 16:1841
9. Yuan JH, Wang K, Xia XH (2005) Adv Funct Mater 15:803
10. Qiu JD, Peng HZ, Liang RP, Li J, Xia XH (2007) Langmuir 23:2133
11. Wang CH, Yang C, Song YY, Gao W, Xia XH (2005) Adv Funct Mater 15:1267
12. Chen W, Xia XH (2007) Chemphyschem 8:1009
13. Meldrum FC, Seshadri R (2000) Chem Commun 1:29
14. Bartlett PN, Birkin PR, Ghanem MA, Toh C-S (2001) J Mater Chem 11:849
15. Briseno AL, Han S, Rauda IE, Zhou F, Toh C-S, Nemanick EJ, Lewis NS (2004) Langmuir 20:219
16. Nikolić ND, Popov KI, Pavlović LjJ, Pavlović MG (2006) J Electroanal Chem 588:88
17. Nikolić ND, Popov KI, Pavlović LjJ, Pavlović MG (2006) Surf Coat Technol 201:560
18. Nikolić ND, Popov KI, Pavlović LjJ, Pavlović MG (2007) J Solid State Electrochem 11:667
19. Nikolić ND, Pavlović LjJ, Pavlović MG, Popov KI (2007) Electrochim Acta 52:8096
20. Nikolić ND, Popov KI, Pavlović LjJ, Pavlović MG (2007) Sensors 7:1
21. Nikolić ND, Pavlović LjJ, Krstić SB, Pavlović MG, Popov KI (2008) Chem Eng Sci 63:2824
22. Nikolić ND, Branković G, Pavlović MG, Popov KI (2008) J Electroanal Chem 621:13
23. Nikolić ND, Popov KI (2010) Hydrogen co-deposition effects on the structure of electrodeposited copper. In: Djokić SS (ed) Electrodeposition: theory and practice, vol 48, Modern aspects of electrochemistry. Springer, New York, pp 1–70
24. Nikolić ND, Maksimović V, Pavlović MG, Popov KI (2009) J Serb Chem Soc 74:689
25. Casas JM, Alvarez F, Cifuentes L (2000) Chem Eng Sci 55:6223
26. Nikolić ND, Pavlović LjJ, Branković G, Pavlović MG, Popov KI (2008) J Serb Chem Soc 73:753
27. Nikolić ND, Pavlović LjJ, Pavlović MG, Popov KI (2007) J Serb Chem Soc 72:1369

28. Amadi A, Gabe DR, Goodenough M (1991) J Appl Electrochem 21:1114
29. Vogt H, Balzer RJ (2005) Electrochim Acta 50:2073
30. Nikolić ND, Branković G, Popov KI (2011) Mater Chem Phys 125:587
31. Kim J-H, Kim R-H, Kwon H-S (2008) Electrochem Commun 10:1148
32. Oniciu L, Muresan L (1991) J Appl Electrochem 21:565
33. Muresan L, Varvara S (2005) Leveling and brightening mechanisms in metal electrodeposition. In: Nunez M (ed) Metal electrodeposition. Nova Science, New York, pp 1–45
34. Popov KI, Maksimović MD (1989) Theory of the effect of electrodeposition at periodically changing rate on the morphology of metal deposition. In: Conway BE, Bockris JO'M, White RE (eds) Modern aspects of electrochemistry, vol 19. Plenum, New York, pp 193–250
35. Popov KI, Djokić SS, Grgur BN (2002) Fundamental aspects of electrometallurgy. Kluwer Academic/Plenum, New York
36. Nikolić ND, Branković G, Pavlović MG, Popov KI (2009) Electrochem Commun 11:421
37. Nikolić ND, Branković G, Maksimović VM, Pavlović MG, Popov KI (2010) J Solid State Electrochem 14:331
38. Popov KI, Nikolić ND, Živković PM, Branković G (2010) Electrochim Acta 55:1919
39. Popov KI, Stojilković ER, Radmilović V, Pavlović MG (1997) Powder Technol 93:55
40. Barton L, Bockris JO'M (1962) Proc Roy Soc A 268:485
41. Nikolić ND, Branković G, Maksimović VM, Pavlović MG, Popov KI (2009) J Electroanal Chem 635:111
42. Ko W-Y, Chen W-H, Tzeng S-D, Gwo S, Lin K-J (2006) Chem Mater 18:6097
43. Popov KI, Pavlović MG (1993) Electrodeposition of metal powders with controlled grain size and morphology. In: White RE, Bockris JO'M, Conway BE (eds) Modern aspects of electrochemistry, vol 24. Plenum, New York, pp 299–391
44. Nikolić ND, Branković G, Maksimović V (2012) J Solid State Electrochem 16:321
45. Nikolić ND, Branković G (2010) Electrochem Commun 12:740
46. Dima GE, de Vooys ACA, Koper MTM (2003) J Electroanal Chem 554–555:15
47. Ko W-Y, Chen W-H, Cheng C-Y, Lin K-J (2009) Sens Actuators B Chem 137:437
48. Pletcher D, Poorbedi Z (1979) Electrochim Acta 24:1253
49. Gorgievski M, Božić D, Stanković V, Bogdanović G (2009) J Hazard Mater 170:716
50. Chandrasekar MS, Pushpavanam M (2008) Electrochim Acta 53:3313
51. Sun BK, O'Keefe TJ (1998) Surf Coat Technol 106:44
52. Nikolić ND, Branković G, Maksimović VM (2011) J Electroanal Chem 661:309
53. Nikolić ND, Branković G (2012) Mater Lett 70:11